Heads and tails: 30 million years of the Afar plume

T. FURMAN[1], J. BRYCE[2], T. ROONEY[1], B. HANAN[3], G. YIRGU[4] & D. AYALEW[4]

[1]*Department of Geosciences, The Pennsylvania State University, University Park, PA 16802, USA (e-mail: furman@geosc.psu.edu)*

[2]*Department of Earth Sciences, University of New Hampshire, Durham, NH 03824, USA*

[3]*Department of Geological Sciences, San Diego State University, San Diego, CA 92182, USA*

[4]*Department of Geological and Geophysical Sciences, Addis Ababa University, Addis Ababa, Ethiopia*

Abstract: Primitive recent mafic lavas from the Main Ethiopian Rift provide insight into the structure, composition and long-term history of the Afar plume. Modern rift basalts are mildly alkalic in composition, and were derived by moderate degrees of melting of fertile peridotite at depths corresponding to the base of the modern lithosphere (*c.*100 km). They are typically more silica-undersaturated than Oligocene lavas from the Ethiopia–Yemen continental flood basalt province, indicating derivation by generally smaller degrees of melting than were prevalent during the onset of plume head activity in this region. Major and trace element differences between the Oligocene and modern suites can be interpreted in terms of melting processes, including melt-induced binary mixing of melts from the Afar plume and those from three mantle end-member compositions (the convecting upper mantle and two enriched mantle sources). The Afar plume composition itself has remained essentially constant over the past 30 million years, indicating that the plume is a long-lived feature of the mantle. The geochemical and isotopic compositions of mafic lavas derived from the Afar plume support a modified single plume model in which multiple plume stems rise from a common large plume originating at great depth in the mantle (i.e. the South African superplume).

Large igneous provinces, including both continental flood basalts (CFB) and oceanic plateaus, represent the largest outpourings of mafic igneous material on our planet. These provinces are attributed to melting associated with the initiation of mantle plume activity (Morgan 1972; White & McKenzie 1995; Richards *et al.* 1989; Hill *et al.* 1992). Several major flood basalt provinces (e.g. Deccan, Paraná–Etendeka, Greenland) have been studied intensively in recent years, leading to the recognition that flood basalt lavas often include contributions from both lithospheric mantle and deep mantle sources, in some cases overprinted by crustal contamination (Hawkesworth *et al.* 1998; Peate *et al.* 1992; Arndt *et al.* 1993; Baker *et al.* 1996*a*, 2000; Fram & Lesher 1997; Janney & Castillo 2001; Ewart *et al.* 2004). It is generally difficult to determine how these source components vary either temporally or spatially, as most flood basalt provinces are either (a) too old/altered to preserve sufficient fresh lavas for detailed geochemical analysis; or (b) deeply dissected by erosion and tectonism associated with the final stages of continental rifting. These difficulties make evaluation of temporal geochemical trends, particularly those associated with the change from plume head magmatism to plume tail activity (e.g. Farnetani *et al.* 2002), unfeasible. The lone exception to these limitations is the Cenozoic Ethiopia–Yemen continental flood basalt province (Fig. 1), the majority of which was emplaced at *c.* 30 Ma and has not yet been compromised by extensive faulting and alteration.

Most studies attribute Ethiopia–Yemen flood basalt activity to impact of the Afar plume head beneath the Ethiopian plateau (e.g. Baker *et al.* 1996*a*; Pik *et al.* 1999; Kieffer *et al.* 2004). The relationship between this copious volcanism at 30 Ma and sparser modern activity in the region is not entirely clear. Most problematic in this regard is the lack of an identifiable track linking the flood basalt province to the modern rift setting that corresponds to plate motion reconstructions. Specifically, it is unresolved whether Africa has been essentially stationary over the past 30 million years (Silver *et al.* 1998; Gripp & Gordon 2002) or whether it has moved north–northeastward over this time period (Gordon & Jurdy 1986; Burke 1996). If modern Afar volcanism is derived from the same plume that fed the Oligocene flood basalts, then geodynamic models must incorporate physical coupling between the plume and the overlying lithosphere (see Calais *et al.* 2006). This issue arises, in part, because Cenozoic volcanism in the East African rift is not limited to the CFB province

From: YIRGU, G., EBINGER, C.J., MAGUIRE, P.K.H. (eds) 2006. *The Afar Volcanic Province within the East African Rift System*. Geological Society, London, Special Publications, **259**, 95–119.
0305-8719/06/$15.00

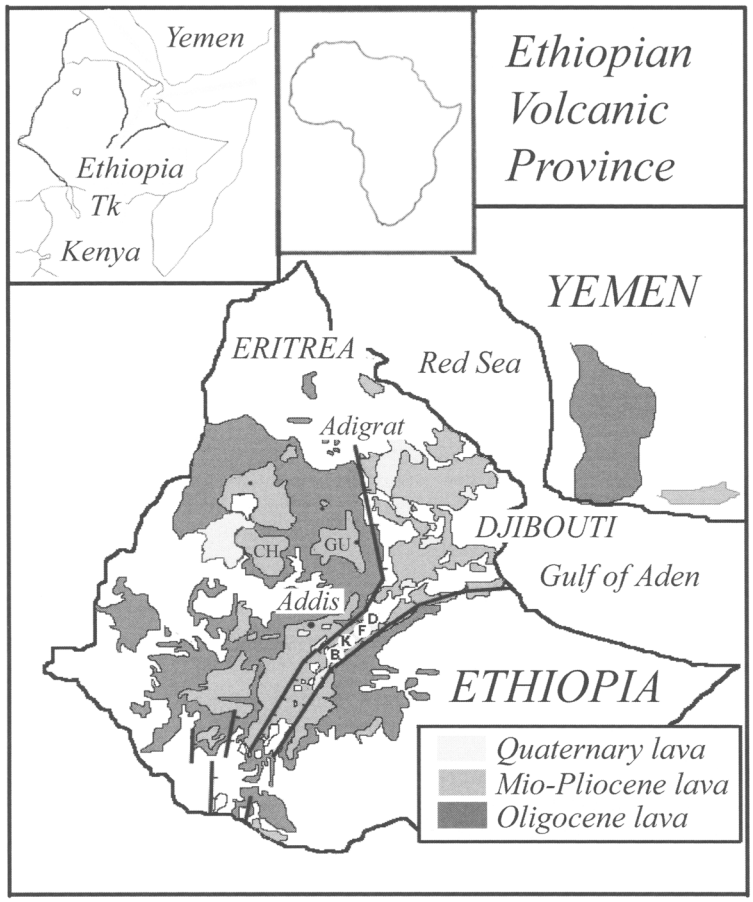

Fig. 1. Map of the Ethiopian Volcanic Province showing ages of volcanic rocks and sample localities mentioned in the text. Recent volcanic centres in the Main Ethiopian Rift are labelled: **D** = Dofan, **F** = Fantale, **K** = Kone, **B** = Boseti. **CH** and **GU** are the 23 Ma volcanic centres of Choke and Guguftu. On the inset map, **Tk** indicates the location of the Turkana province.

in Ethiopia and Yemen. In southernmost Ethiopia, voluminous basaltic activity began at *c.* 45 Ma, about 15 million years prior to the inferred arrival of the Oligocene plume head at the base of the Ethiopian lithosphere (Davidson & Rex 1980; Haileab *et al.* 2004; Vetel & Le Gall 2006). This dual-focus distribution of thick basalt sequences characterized by a variety of compositional differences has led to a range of geodynamic models involving both single (Ebinger & Sleep 1998), modified single (Furman *et al.* 2004, 2006) and double (George *et al.* 1998; Rogers *et al.* 2000; Pik *et al.* 2006; Rogers 2006) plumes, the validity of which remain unresolved. Most recently, volcanism in Afar and throughout East and South Africa has been attributed to the South African superplume (Janney *et al.* 2002; Kieffer *et al.* 2004; Furman *et al.* 2004, 2006), the largest seismic anomaly in the deep mantle (e.g. Ritsema *et al.* 1999; Gurnis *et al.* 2000; Nyblade *et al.* 2000; Zhao 2001; Ni *et al.* 2002). If our analysis indicates that the Afar plume has been a consistent feature of the deep mantle for 30 million years, it will provide a new window into the thermochemical structure of the South African superplume and its long-term evolution.

In this paper, we present new geochemical data on young mafic lavas from the Main Ethiopian Rift. These data permit characterization of the melting conditions and source components as they vary temporally. We then integrate our findings with the geochemical signatures from Oligocene and recent mafic lavas over the spatial extent of the CFB province. We combine data from several

well-constrained regional studies from the Yemeni and Ethiopian portions of the Oligocene flood basalt sequences, and compare them to recent volcanics from Djibouti, the Afar region, the Main Ethiopian Rift and the Turkana province. The new data, taken in context with the CFB data, provide constraints on several outstanding questions relevant to flood basalt petrogenesis, namely: (a) What are the conditions of mantle melting at the onset of plume activity? (b) What source domains are involved in the genesis of the Oligocene magmas? (c) Do these same characteristics persist until the present time? (d) Is the Afar plume a long-lived feature of the mantle?

Geodynamic setting

The Cenozoic Ethiopia–Yemen flood basalt province is located at the junction of three rifts: the Red Sea, the Gulf of Aden, and the East African rift system. Within central Ethiopia and Eritrea, the flood basalts cover an area of about 600 000 km^2, with an estimated total volume of about 350 000 km^3 (Mohr 1983; Mohr & Zanettin 1988). The lava pile thickness varies, reaching up to 2000 m along the margins of the southern Red Sea, and thinning to about 500 m towards both north and south. Most of the basalts and associated felsic rocks were erupted in a period of *c.*1 million years at around 30 Ma (Zumbo *et al.* 1985; Baker *et al.* 1996*b*; Hofmann *et al.* 1997; Pik *et al.* 1998), concomitant with the onset of continental rifting by 29 Ma (Wolfenden *et al.* 2004). This continental flood basalt province contains the youngest and best-exposed sequence of mafic volcanic rocks associated with incipient continental break-up. It has been an area of episodic magmatic activity since the Oligocene, and is today a site of mafic volcanism attributed to the Afar plume (Vidal *et al.* 1991; Schilling *et al.* 1994; Marty *et al.* 1993, 1996; Deniel *et al.* 1994; Barrat *et al.* 1998). The Ethiopian continental flood basalt province thus provides an excellent opportunity to evaluate questions related to plume magmatism throughout the process of incipient continental rifting.

Detailed geochemical studies of modern hotspot volcanism in Hawaii (Lassiter & Hauri 1998; Blichert-Toft *et al.* 1999; DePaolo *et al.* 2001; Abouchami *et al.* 2005; Bryce *et al.* 2005), the Galápagos (Hoernle *et al.* 2000; Harpp & White 2001; Geldmacher *et al.* 2003; Thompson *et al.* 2004) and Iceland (Thirlwall 1995; Fitton *et al.* 1997; Hanan & Schilling 1997; Hanan *et al.* 1999; Kempton *et al.* 2000) have demonstrated convincingly that long-lived heterogeneities are preserved within mantle plumes located in ocean basins. These heterogeneities are expressed, to first order, spatially and/or temporally on these oceanic islands and thus are thought to represent melting of long-lived chemical and mineralogical domains located within the source region of the plume tail. No comparable study of spatial and temporal variations in plume volcanism has been attempted in a continental setting. The Afar plume provides an ideal laboratory to test these ideas using fairly young lavas (<30 Ma) from a tectonic environment that is well-constrained in both structural and geophysical terms (e.g. Mahatsente *et al.* 1999; Benoit *et al.* 2003; Keranen *et al.* 2004; Dugda *et al.* 2005; Kendall *et al.* 2005; Mackenzie *et al.* 2006; Bastow *et al.* 2005).

The mafic lavas in this study were collected from four volcanic centres within the Wonji Fault Belt (Mohr 1962; WoldeGabriel *et al.* 1990); from north to south they are Dofan, Fantale, Kone and Boseti (Fig. 1). Each volcano has a well-developed central silicic volcanic edifice, with basaltic lavas erupted primarily from cinder cones and along fissures towards the volcano flanks and between the volcanoes. At Kone, basaltic fissures cut through the nested Quaternary caldera structures and continue to the SW. These silicic volcanoes have been active for about three million years (WoldeGabriel *et al.* 1990; Chernet & Hart 1999) and have had several catastrophic eruptions which produced the pumice and ash that cover the rift valley floor.

Sampling

Samples in this study were collected during field excursions in 2002 and 2003 and were chosen to obtain representative coverage of mafic lavas from the individual Quaternary volcanoes, augmented by post-Miocene syn-rift basalts emplaced along the border faults. This investigation is thus more comprehensive than previous studies that have broader regional coverage and/or include samples that range from Oligocene to Recent (Hart *et al.* 1989; Boccaletti *et al.* 1999; Chernet & Hart 1999). We focus here on fresh, young mafic lavas with >6 wt% MgO in order to elucidate the history of mantle melting and the nature of the source domains that contribute to this modern volcanism. The origin of more-evolved lavas (samples with <6 wt% MgO), including a discussion of shallow-level fractionation processes and its relationship to magmatic segmentation of the rift axis, will be presented elsewhere. The basalts are sparsely phyric, typically with <5 vol.% phenocrysts of olivine, accompanied in more-evolved basalts by clinopyroxene and plagioclase in variable proportions.

In order to assess the chemical heterogeneity within the modern volcanic province, we incorporate studies of mafic lavas from Djibouti (Vidal *et al.* 1991; Deniel *et al.* 1994), Erta 'Ale (Barrat *et al.* 1998; Ayalew *et al.* unpublished data) and the West Sheba Ridge in the Gulf of Aden (Schilling *et al.* 1992). To evaluate possible temporal evolution of the Afar plume, we compare these recent basalt suites to well-documented Oligocene continental flood basalts from Ethiopia (Pik *et al.* 1998, 1999; Kieffer *et al.* 2004) and Yemen (Chazot & Bertrand 1993; Baker *et al.* 1996*a*, 2000). There are limited data available for lavas emplaced between 30 and 3 Ma; we include analyses of the *c.*7 Ma Addis Ababa series (this study) and 23 Ma basalts from Choke and Guguftu volcanoes (Kieffer *et al.* 2004; Fig. 1). To broaden our regional scope, we compare the Afar province lavas to basalts from Turkana, nothern Kenya (Furman *et al.* 2004, 2006); geochemical characteristics of the Kenya rift are described elsewhere (Rogers 2006).

Analytical methods

Centimetre-thick slabs were polished to remove saw marks, and then crushed into millimetre-sized chips. These chips were then powdered in a WC disc mill. Bulk rock analyses for major and trace elements were completed by DCP and ICP-MS analysis at Duke University and by ICP-MS at the Centre Récherches Pétrographiques et Géochimiques, Nancy, France (Table 1). Bulk rock Sr–Nd–Pb isotopic analyses (Table 2) were performed at UCLA and San Diego State University. Details of the analytical procedures are in the Appendix.

Results

Major elements

The modern Ethiopian rift lavas comprise primarily transitional tholeiitic basalts and trachybasalts (Fig. 2). Their bulk compositions are hypersthene- to mildly nepheline-normative, and evolved lavas tend towards silica-undersaturated compositions. The Ethiopian lavas are thus compositionally similar to contemporaneous mafic lavas from Turkana, northern Kenya (Furman *et al.* 2004) and 23 Ma basalts from Choke and Guguftu, but more alkali-rich than the Oligocene flood basalts which are dominated by quartz-normative tholeiites (Pik *et al.* 1999; Kieffer *et al.* 2004). The degree of differentiation of recent lavas varies between the individual volcanoes, with the most primitive basalts erupted from fissures immediately south of Kone. Each of the central volcanic complexes is characterized by low-MgO basalts through rhyolitic lavas.

The majority of lavas described in this study contain between 6.5 and 9.5 wt% MgO; no picritic lavas have been sampled in the modern rift setting although rare Fe-rich picrites (ferropicrites of Gibson *et al.* 2000) occur in both Ethiopian and Yemeni flood basalt sequences. Recent Ethiopian basalts have TiO_2 contents that range from 1.8–2.3 wt%, somewhat higher than values observed among Oligocene low-Ti lavas (1.1–2.1 wt%) but substantially lower than the primitive high-Ti suite (2.7–5.1 wt%). Pik *et al.* (1999) identified these coeval high- and low-titanium basalt series within the continental flood basalt sequence, and proposed a geographic control on eruptive composition. The presence of sparse high-Ti lavas among the Yemeni flood basalt sequence (Baker *et al.* 1996*b*), however, suggests that this lava type is more widespread than recognized previously.

Trace elements

Abundances of compatible trace elements approach those expected for primary mantle melts (*c.* 200 ppm Ni, *c.* 750 ppm Cr, *c.* 33 ppm Sc; Table 1), suggesting that the most magnesian modern Ethiopian rift lavas have undergone only minor olivine fractionation during melt ascent and storage. Variation of these elements with MgO content among primitive Ethiopian basalts of all ages suggests a dominant role for olivine crystallization; in contrast, co-precipitation of olivine and clinopyroxene is inferred for Quaternary basalts from Turkana, nothern Kenya (Furman *et al.* 2004).

Chondrite-normalized rare earth element (REE) patterns of the Ethiopian rift basalts have moderate negative slopes and show little variation within or between eruptive centres (Fig. 3). Oligocene flood basalts from throughout Ethiopia (Pik *et al.* 1999) have lower overall abundances and consistently flatter rare earth element patterns, whereas primitive high-Ti samples have steeper patterns and substantially higher abundances, despite their higher MgO contents (Fig. 3). Two Oligocene high-Ti lavas from Adigrat (NW Ethiopia) have moderately steep, concave-down patterns that set them apart from the other flood basalts. In contrast to all of the Oligocene lavas, the 23 Ma lavas from Choke and Guguftu have rare earth element abundances that fall within the range of the modern rift lavas (Fig. 3), consistent with major element evidence (Fig. 2) suggesting these lavas are more closely related to Quaternary Turkana basalts than to the CFB and Main Ethiopian Rift products.

Incompatible trace element abundances in the young Ethiopian rift basalts are moderately

Table 1. *Major amd trace element and isotopic data for Ethiopian rift basalts. See supplementary data section in the Appendix for analytical techniques, precision and accuracy. The isotopic data presented for the 7 Ma Addis Ababa samples (denoted with*) represent initial values. The Δ8/4 values are computed according to Hart (1984); the NHRL model values are corrected to 7 Ma values using κ = 2.5.*

Sample	1027	1023	1018	E99-2	1032	N-18	1035	1035A	N-17	E99-3	1030
Location	Dofan	Dofan	Fantale	Fantale	Fantale	Fantale	Fantale	Fantale	Kone	Kone	Kone
Latitude (N)	9.48	9.14	8.92		8.87	8.91	8.80	8.80	8.88		8.89
Longitude (E)	40.20	39.95	39.84		39.91	39.83	39.68	39.68	39.79		39.79
SiO_2	46.78	46.15	46.88	46.52	47.48	46.26	47.28	46.41	46.64	46.68	47.00
Al_2O_3	15.73	15.75	16.26	16.72	16.25	15.63	15.48	15.64	16.37	16.58	16.33
TiO_2	2.25	2.20	2.58	2.46	2.47	2.24	2.31	2.26	2.71	2.41	2.33
Fe_2O_3	12.77	12.45	13.46	13.14	12.88	12.06	12.52	12.34	14.27	13.23	13.00
MgO	7.35	8.08	6.23	6.35	6.65	7.35	7.68	7.80	6.27	6.65	6.83
MnO	0.19	0.18	0.21	0.20	0.20	0.19	0.19	0.18	0.21	0.19	0.20
CaO	11.00	11.60	9.13	9.48	9.62	10.78	11.14	10.87	9.04	10.41	10.00
Na_2O	2.68	2.41	3.41	3.36	3.33	3.20	2.85	2.90	3.34	3.09	3.10
K_2O	0.58	0.77	1.01	1.12	0.93	1.12	0.71	0.68	0.98	0.76	0.78
P_2O_5	0.42	0.40	0.61	0.52	0.57	0.50	0.44	0.42	0.50	0.41	0.38
Sum	99.75	99.99	99.78	99.87	100.38	99.32	100.60	99.50	100.32	100.41	99.95
Cs	0.05	0.09	0.08	0.34	0.11	0.11	0.08	0.10	0.04	0.17	0.06
Rb	10.6	16.4	13.8	18.2	15.9	17.0	12.3	14.6	11.4	9.9	10.7
Ba	235	308	504	456	465	414	288	279	428	343	357
Th	1.59	1.91	1.46	2.09	1.56	2.01	1.29	1.45	1.61	1.56	1.43
U	0.4	0.4	0.5	0.5	0.4	0.5	0.4	0.4	0.4	0.2	0.4
Nb	27.4	28.8	33.7	29.8	29.7	32.2	22.7	23.2	32.9	22.0	23.2
Ta	1.7	1.7	2.0	2.0	1.8	1.9	1.4	1.4	2.0	1.5	1.5
Pb	1.7	1.6	2.4	2.4	2.3	2.2	2.0	2.1	2.0	1.5	1.6
Sr	382	591	411	539	522	497	415	462	479	487	448
Zr	190	124	157	168	150	155	121	125	169	129	132
Hf	4.4	2.9	3.6	3.3	3.5	3.6	2.8	2.9	4.2	2.8	3.4
Y	28.5	24.8	28.6	27.4	27.3	27.6	25.9	24.7	27.2	23.1	23.9
Co	66.6	50.0	47.6	47.9	45.3	46.7	47.6	50.3	47.6	48.2	65.6
Cr	172	221	38	58	64	214	218	232	30	106	89
Ni	91	86	44	43	64	82	84	82	49	57	62
V	350	298	287	286	273	277	313	306	300	300	283
Sc	32.1	26.5	20.7	25.4	31.2	27.9	30.9	30.3	27.5	31.0	31.3
La	20.3	18.9	20.8	27.3	22.2	24.6	15.3	17.1	23.1	19.7	19.2
Ce	44.9	41.3	50.6	59.4	50.6	52.5	35.8	38.6	51.9	45.2	41.7
Pr	3.0	5.3	6.2	6.9	6.7	6.6	4.5	5.1	6.5	5.2	5.5

(*continued*)

Table 1. *Continued*

Sample	1027	1023	1018	E99-2	1032	N-18	1035	1035A	N-17	E99-3	1030
Location	Dofan	Dofan	Fantale	Fantale	Fantale	Fantale	Fantale	Fantale	Kone	Kone	Kone
Nd	25.4	21.9	25.9	30	28.5	28.4	19.4	21.3	28.5	23.3	23.5
Sm	5.67	4.82	5.50	6.34	6.20	5.97	4.31	4.69	6.24	5.17	5.26
Eu	2.02	1.74	2.09	2.36	2.32	2.13	1.54	1.73	2.27	1.89	1.98
Gd	5.96	5.10	5.88	6.17	6.35	6.46	4.56	5.09	6.68	4.79	5.34
Tb	0.96	0.73	0.84	0.89	0.92	1.01	0.68	0.75	1.07	0.72	0.84
Dy	5.34	4.02	4.47	4.84	5.05	5.05	3.73	4.16	5.35	4.17	4.58
Ho	1.07	0.78	0.87	0.93	0.97	0.99	0.71	0.82	1.02	0.78	0.93
Er	2.82	2.03	2.28	2.37	2.45	2.61	1.86	2.11	2.75	2.00	2.32
Yb	2.51	1.77	1.96	2.14	2.18	2.25	1.67	1.88	2.37	1.90	2.06
Lu	0.37	0.27	0.29	0.32	0.33	0.34	0.25	0.27	0.36	0.28	0.32
$^{87}Sr/^{86}Sr$	0.703722	0.704102	—	0.704117	—	0.703961	0.704198	—	—	—	—
$^{143}Nd/^{144}Nd$	0.512862	0.512817	—	0.512798	—	0.512799	0.512767	—	—	—	—
ε_{Nd}	4.4	3.5	—	3.1	—	3.1	2.5	—	—	—	—
$^{206}Pb/^{204}Pb$	18.827	18.752	—	—	—	18.732	18.627	—	—	—	—
$^{207}Pb/^{204}Pb$	15.581	15.584	—	—	—	15.597	15.585	—	—	—	—
$^{208}Pb/^{204}Pb$	38.896	38.782	—	—	—	38.834	38.748	—	—	—	—
$\Delta 8/4$	50.72	48.38	—	—	—	56.00	60.10	—	—	—	—

Sample	N-16	N-22	KO-12	N-20	1037	N-15	1036	E99-11	KO-4B	N-21
Location	Kone	Kone	Kone	Kone	Kone	Kone	Kone	Kone	Kone	Kone
Latitude (N)	8.84	8.72		8.83	8.86	8.78	8.84			8.78
Longitude (E)	39.70	39.68		39.69	39.75	39.63	39.71			39.68
SiO_2	46.14	45.42	46.53	45.86	47.14	46.35	46.50	46.28	46.43	46.86
Al_2O_3	15.91	15.29	15.58	14.86	15.06	14.89	14.78	15.03	14.75	14.10
TiO_2	2.46	2.31	2.27	2.21	1.95	2.22	2.20	2.14	2.17	1.90
Fe_2O_3	12.82	12.43	12.65	12.46	11.92	12.18	12.56	12.42	12.55	11.73
MgO	6.83	7.97	8.14	8.33	8.35	8.64	8.51	8.78	8.85	10.44
MnO	0.19	0.19	0.18	0.19	0.19	0.19	0.20	0.17	0.19	0.18
CaO	10.95	11.19	10.78	10.58	10.17	10.91	10.69	11.37	10.74	11.02
Na_2O	3.06	3.12	2.89	3.25	2.87	2.73	3.21	2.70	3.22	2.82
K_2O	0.82	1.13	0.64	1.12	0.88	1.06	1.07	0.65	1.00	0.67
P_2O_5	0.45	0.55	0.60	0.54	0.46	0.45	0.55	0.33	0.60	0.37
Sum	99.63	99.61	100.26	99.41	98.99	99.61	100.27	99.87	100.50	100.09
Cs	0.13	0.34	0.15	0.26	0.09	0.15	0.19	0.12	0.33	0.13

Rb	13.1	28.2	12.2	23.6	12.7	18.4	22.2	11.2	26.7	12.7
Ba	299	405	272	391	401	324	411	241	357	246
Th	1.57	3.25	1.57	2.69	1.63	2.04	2.30	1.84	2.97	1.41
U	0.4	0.9	0.3	0.8	0.4	0.5	0.8	0.4	0.7	0.4
Nb	24.9	47.3	18.7	40.8	29.6	30.2	41.3	20.6	33.0	22.9
Ta	1.5	2.7	1.5	2.3	1.8	1.7	2.4	1.5	2.5	1.3
Pb	2.0	2.3	3.0	2.6	2.0	2.0	2.6	1.7	3.0	3.2
Sr	521	619	488	586	479	468	404	427	526	392
Zr	141	175	122	164	148	138	158	125	148	141
Hf	3.4	3.7	3.1	3.7	3.7	3.2	3.5	3.0	3.5	3.6
Y	25.7	27.1	21.4	25.5	27.0	24.1	27.8	21.2	23.2	23.5
Co	48.8	52.0	51.3	50.2	61.3	49.6	47.7	54.0	50.1	54.1
Cr	143	204	289	339	292	345	309	465	433	556
Ni	73	96	109	135	118	145	123	160	141	165
V	302	287	300	259	256	293	277	287	283	287
Sc	31.0	31.3	29.4	30.7	32.4	17.7	33.4	29.4	33.5	24.7
La	19.2	31.5	18.6	28.2	23.9	20.2	22.9	17.7	27.9	17.0
Ce	42.2	64.4	40.2	57.9	51.7	42.8	51.9	40.7	57.3	37.1
Pr	5.5	7.7	5.2	7.0	6.8	5.3	6.1	4.7	7.0	4.8
Nd	24.2	31.6	22.6	29.3	28.8	23.2	24.1	20.6	28	21.1
Sm	5.19	6.16	5.28	5.70	6.28	4.84	4.98	4.64	5.73	4.50
Eu	1.87	2.05	1.85	1.99	2.12	1.67	1.62	1.71	1.82	1.61
Gd	5.73	6.51	4.75	6.20	5.81	5.22	5.09	4.45	5.53	4.89
Tb	0.91	1.01	0.70	0.95	0.93	0.85	0.72	0.67	0.76	0.81
Dy	4.74	4.98	3.90	4.65	5.10	4.31	3.84	3.73	4.52	4.21
Ho	0.92	0.96	0.80	0.90	1.00	0.85	0.72	0.76	0.84	0.81
Er	2.38	2.53	1.91	2.44	2.63	2.27	1.91	2.01	2.30	2.21
Yb	2.17	2.09	1.73	2.05	2.34	1.96	1.67	1.78	1.90	2.04
Lu	0.31	0.32	0.31	0.31	0.35	0.30	0.24	0.28	0.31	0.29
$^{87}Sr/^{86}Sr$	—	0.703768	0.704303	0.703996	0.704251	0.704203	0.703949	—	0.704015	0.704228
$^{143}Nd/^{144}Nd$	—	0.512838	0.512765	—	0.512768	0.512800	0.512799	—	0.512801	0.512793
ε_{Nd}	—	3.9	2.5	—	2.5	3.2	3.1	—	3.2	3.0
$^{206}Pb/^{204}Pb$	—	18.945	18.658	18.811	18.557	18.680	18.808	—	18.801	18.624
$^{207}Pb/^{204}Pb$	—	15.595	15.593	15.592	15.584	15.588	15.590	—	15.596	15.586
$^{208}Pb/^{204}Pb$	—	38.896	38.826	38.873	38.632	38.879	38.862	—	38.872	38.794
$\Delta 8/4$	—	36.45	64.15	50.35	56.96	66.79	49.61	—	51.46	65.06

(*continued*)

Table 1. *Continued.*

Sample Location	E99-6 Kone	N-02 Boseti	N-01 Boseti	E99-13 Boseti	E99-20 Boseti	N-12 E. Rift Wall	N-09 E. Rift Wall	W-04 E. Rift Flank	E01-15A W. Rift Flank
Latitude (N)		8.44	8.39			8.28	8.26		8.92
Longitude (E)		39.40	39.33			39.41	39.50		39.55
SiO_2	47.11	47.14	46.78	47.37	46.87	50.59	48.53	45.05	47.52
Al_2O_3	14.51	15.50	14.65	15.15	15.09	16.32	15.49	16.94	15.60
TiO_2	1.82	2.20	2.15	2.16	2.20	2.20	1.54	2.57	2.42
Fe_2O_3	11.59	11.98	11.96	12.09	12.16	11.83	11.42	12.63	14.54
MgO	10.66	7.60	8.46	8.46	9.13	5.95	8.63	7.25	5.74
MnO	0.18	0.18	0.18	0.18	0.18	0.18	0.19	0.18	0.21
CaO	11.16	10.31	11.10	11.35	11.25	8.97	9.62	11.49	8.50
Na_2O	2.54	3.02	2.75	2.79	2.65	3.21	3.36	2.41	3.27
K_2O	0.63	1.04	0.90	0.77	0.66	1.32	1.02	0.75	0.96
P_2O_5	0.35	0.58	0.50	0.48	0.39	0.44	0.41	0.39	0.53
Sum	100.55	99.55	99.43	100.80	100.58	101.00	100.18	99.66	99.29
Cs	0.26	0.11	0.10	0.41	0.06	0.16	0.24	0.05	0.22
Rb	12.1	13.1	14.0	24.6	10.9	14.6	16.0	11.0	21.5
Ba	240	437	373	662	291	504	371	200	497
Th	1.80	1.94	1.68	3.93	1.90	1.98	1.69	1.62	2.52
U	0.4	0.4	0.5	0.9	0.3	0.5	0.4	0.5	0.5
Nb	19.7	30.5	27.0	42.0	20.2	27.9	22.4	24.4	22.0
Ta	1.4	1.8	1.6	2.8	1.5	1.6	1.3	1.5	1.3
Pb	1.9	2.7	2.5	4.7	2.2	4.3	5.8	1.6	4.2
Sr	399	501	470	730	471	587	523	468	440
Zr	117	176	146	215	125	210	131	148	190
Hf	2.7	3.9	3.2	4.4	2.8	4.8	3.2	3.5	4.5
Y	20.5	26.6	23.7	26.9	20.6	32.2	24.4	23.0	41.4
Co	54.7	46.7	49.5	61.8	50.3	44.7	44.0	47.1	49.0
Cr	757	240	342	721	540	60	336	40	49
Ni	209	97	109	202	141	47	135	72	64
V	276	260	278	250	279	227	217	267	322
Sc		29.4	33.5			24.7	27.3	27.8	30.8
La	17.5	25.5	22.0	40.7	18.8	26.4	18.7	18.1	26.0
Ce	38.9	53.8	47.2	86.8	41.7	58.0	39.7	40.5	52.7
Pr	4.5	6.9	6.0	10.0	5.1	7.4	5.0	5.4	7.1
Nd	20.4	28.9	25.4	41.9	22	31.4	21.2	22.6	30.7
Sm	4.37	5.89	5.31	8.50	4.79	6.27	4.43	5.05	6.75
Eu	1.58	2.11	1.88	2.71	1.81	2.02	1.50	1.81	2.17

Gd	4.16	6.31	5.64	7.17	4.61	6.94	5.04	5.22	7.43
Tb	0.68	0.96	0.90	0.95	0.63	1.11	0.81	0.82	1.19
Dy	3.74	4.85	4.45	4.93	3.76	5.76	4.31	4.37	6.80
Ho	0.77	0.97	0.83	0.92	0.71	1.12	0.86	0.85	1.39
Er	1.90	2.48	2.21	2.14	1.89	3.03	2.32	2.18	3.81
Yb	1.78	2.20	1.97	2.01	1.76	2.79	2.16	1.87	3.40
Lu	0.27	0.33	0.28	0.30	0.24	0.42	0.31	0.28	0.52
$^{87}Sr/^{86}Sr$	—	—	0.704485	—	0.704117	0.704982	0.704255	—	—
$^{143}Nd/^{144}Nd$	—	—	0.512730	—	—	0.512585	0.512695	—	—
ε_{Nd}	—	—	1.8	—	—	−1.0	1.1	—	—
$^{206}Pb/^{204}Pb$	—	—	18.518	—	18.694	17.853	18.836	—	—
$^{207}Pb/^{204}Pb$	—	—	15.589	—	15.591	15.578	15.620	—	—
$^{208}Pb/^{204}Pb$	—	—	38.686	—	38.791	38.181	38.854	—	—
$\Delta 8/4$	—	—	67.07	—	56.30	96.97	45.43	—	—

Sample Location	E01-20 W. Rift Flank	E01-32 Awash Gorge	E-43 W. Rift Flank	AA99-10* Addis Ababa	AA99-6* Addis Ababa	AA99-03* Addis Ababa	AA99-19 Addis Ababa
Latitude (N)	9.02	8.88	9.13				
Longitude (E)	39.56	40.10	39.73				
SiO_2	48.93	47.09	47.74	45.12	46.14	47.67	48.49
Al_2O_3	15.01	16.20	15.37	13.05	14.11	15.11	17.17
TiO_2	2.50	2.22	3.09	1.50	1.61	2.26	1.94
Fe_2O_3	13.60	13.06	13.05	11.25	12.79	12.53	11.59
MgO	5.97	6.49	7.20	14.38	12.14	8.40	6.36
MnO	0.21	0.23	0.18	0.16	0.18	0.18	0.16
CaO	10.35	11.09	9.25	11.06	9.11	9.80	9.69
Na_2O	3.25	2.95	3.19	2.32	3.02	2.94	3.25
K_2O	0.72	0.56	1.21	0.63	0.74	1.08	0.91
P_2O_5	0.46	0.37	0.51	0.26	0.32	0.59	0.38
Sum	101.00	100.26	100.79	99.73	100.16	100.56	99.94
Cs	8.8	0.010.07	0.43	0.28	0.25	0.03	0.23
Rb	330	7.7	26.8	15.4	15.8	13.9	18.2
Ba	1.64	364	405	236	294	379	320
Th	0.1	1.14	3.39	2.20	1.73	1.88	2.33
U	24.7	0.3	0.9	0.5	0.3	0.2	0.4
Nb	1.5	17.9	44.6	23.6	27.4	32.8	22.7
Ta	2.2	1.1	2.8	1.7	2.0	1.9	1.5
Pb	457	1.8	3.4	1.9	2.4	3.2	3.2
Sr	154	470	694	454	361	544	636

(*continued*)

Table 1. *Continued*

Sample Location	E01-20 W. Rift Flank	E01-32 Awash Gorge	E-43 W. Rift Flank	AA99-10* Addis Ababa	AA99-6* Addis Ababa	AA99-03* Addis Ababa	AA99-19 Addis Ababa
Zr	3.6	127	269	99	144	174	133
Hf	28.3	2.9	5.9	2.5	2.9	4.0	2.9
Y	45.1	24.7	30.8	17.9	26.2	28.4	22.4
Co	52	47.5	54.0	64.7	64.3	58.2	44.9
Cr	50	45	109	1136	663	391	64
Ni	313	73	72	410	389	124	35
V	32.5	281	281	234	218	258	272
Sc	19.8	29.9	23.9	30.8		30.8	
La	45.0	15.9	33.9	17.4	19.6	27.4	20.7
Ce	5.9	35.3	47.8	36.7	36.1	61.5	44.2
Pr	25.8	4.8	9.7	4.3	4.4	7.5	5.3
Nd	8.53	20.9	39.7	17.8	18.3	30.9	23
Sm	2.01	4.80	8.27	3.67	3.93	6.33	4.86
Eu	6.06	1.76	2.71	1.27	1.33	2.11	1.63
Gd	0.96	5.12	8.15	4.01	3.94	6.54	4.53
Tb	5.21	0.82	1.17	0.57	0.61	0.99	0.65
Dy	1.02	4.40	5.93	3.06	3.47	5.21	3.92
Ho	2.69	0.90	1.13	0.70	0.67	1.02	0.74
Er	2.36	2.37	2.86	1.60	1.83	2.57	1.93
Yb	0.34	2.17	2.32	1.64	1.81	2.33	1.96
Lu	0.704237	0.32	0.33	0.21	0.28	0.35	0.28
$^{87}Sr/^{86}Sr$	0.512753	0.704321	0.703841	0.703643	0.703880	0.704064	—
$^{143}Nd/^{144}Nd$	2.2	0.512767	0.512842	0.512886	0.512780	0.512748	—
ε_{Nd}		2.5	4.0	4.8	2.8	2.1	—
$^{206}Pb/^{204}Pb$	—	18.429	18.837	18.779	—	18.212	—
$^{207}Pb/^{204}Pb$	—	15.580	15.597	15.594	—	15.570	—
$^{208}Pb/^{204}Pb$	—	38.540	38.851	38.769	—	38.398	—
$\Delta 8/4$	—	63.23	45.01	43.74	—	75.19	—

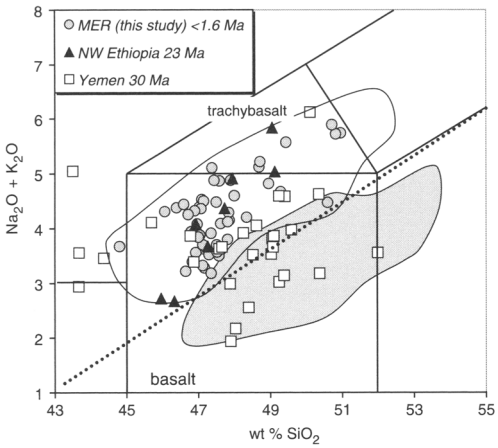

Fig. 2. The total alkalis–silica classification diagram for mafic volcanics of the Ethiopia–Yemen CFB province shows consistent temporal variations. Data are recalculated to 100% on an anhydrous basis with $Fe^{3+} = 15\%$ of total iron; the dotted line is the alkalic–tholeiitic division of Macdonald & Katsura (1964) for Hawaiian lavas. Mildly alkalic basalts from the modern Main Ethiopian Rift (MER samples from this study shown as data points; field includes data from Hart *et al.* 1989; Boccaletti *et al.* 1999; Chernet & Hart 1999) define a range distinct from that of tholeiitic 30 Ma Ethiopian lavas (shaded field; Hart *et al.* 1989; Pik *et al.* 1999; Kieffer *et al.* 2004). Yemeni CFBs (Chazot & Bertrand 1993; Baker *et al.* 1996*b*) generally overlap the Ethiopian suite but include samples with higher alkali contents. Note that 23 Ma basalts from NW Ethiopia (Kieffer *et al.* 2004) plot within the modern MER field.

enriched over primitive mantle (Sun & Mcdonough 1989), and generally overlap values measured in recent Djibouti lavas attributed to the Afar plume (Vidal *et al.* 1991; Deniel *et al.* 1994). Normalized incompatible trace element variation diagrams (Fig. 3) show generally parallel patterns within the Ethiopian rift suite: all samples have prominent positive Ba and Nb–Ta anomalies and weakly negative K anomalies. In detail, however, some consistent differences are found between lavas from individual volcanic centres that require distinct histories of melting and/or a limited degree of source heterogeneity along the rift axis. For example, MgO-rich Kone basalts have the highest abundances of most highly incompatible trace elements, suggesting these lavas are derived by a lower degree of melting than occurs beneath neighbouring volcanoes; this observation is consistent with the higher normative nepheline contents of those same lavas.

Regional and temporal differences observed among incompatible trace element abundances provide insight into the source regions of the mafic lavas through space and time (Fig. 3). Recent Djibouti basalts have slightly lower abundances of the most highly incompatible elements and P, but otherwise define patterns that parallel those of modern Main Ethiopian Rift lavas. Primitive Oligocene high-Ti lavas from Ethiopia and Yemen, including Adigrat, have abundances of the most highly incompatible trace elements that generally overlap the Ethiopian rift suite, but the older samples lack Ba anomalies and have consistently higher abundances of the middle and heavy REE, Zr, Hf, Ti and Y (Pik *et al.* 1999). In contrast, Oligocene lavas with <7 wt% MgO have lower contents of the more highly incompatible elements than the Ethiopian rift lavas, and overlapping abundances of the moderately incompatible elements (Fig. 4). Most of these suites are characterized by lavas with positive Ba anomalies (leading to elevated Ba/Rb) and negative K anomalies that suggest melting in the presence of minor amphibole.

Mafic Ethiopian rift lavas define a restricted range in La/Nb–Ba/Nb that is close to primitive mantle values, indicating a limited role for enriched mantle or mantle lithosphere sources (Fig. 4). Many of the Ethiopian rift basalts plot within the field defined by recent lavas derived from the Afar plume as sampled in Djibouti and Erta' Ale. Primitive high-Ti Oligocene lavas overlap these fields at low Ba/Nb values, but moderate- and low-Ti flood basalts from both Ethiopia and Yemen extend to much higher values of La/Nb and Ba/Nb, indicating a substantial contribution from enriched mantle sources. Similarly, Ce/Pb values of the Ethiopian rift and primitive high-Ti lavas plot primarily within the range of mantle-derived basalts, whereas the other suites trend towards both crustal and lithospheric end-members (Fig. 4). This ratio is influenced by crustal contributions, as Pb is elevated in crustal rocks relative to mantle lithologies, and the Ce/Pb value of mantle-derived liquids is well constrained (25 ± 5; Hofmann *et al.* 1986). It is interesting to note that Yemen flood basalts that plot within the field of modern rift lavas in Fig. 2 have consistently low values of Ce/Pb (<10) that suggest crustal contamination has played a role in elevating their alkali abundances.

Radiogenic isotopic data

Radiogenic isotope signatures of recent Ethiopian rift basalts (Table 1) indicate along-axis variations in source composition and/or melt generation processes, and probably also reflect variations in both crustal stretching (Maguire *et al.* 2006) and lithospheric thinning (Bastow *et al.* 2005). Lavas from

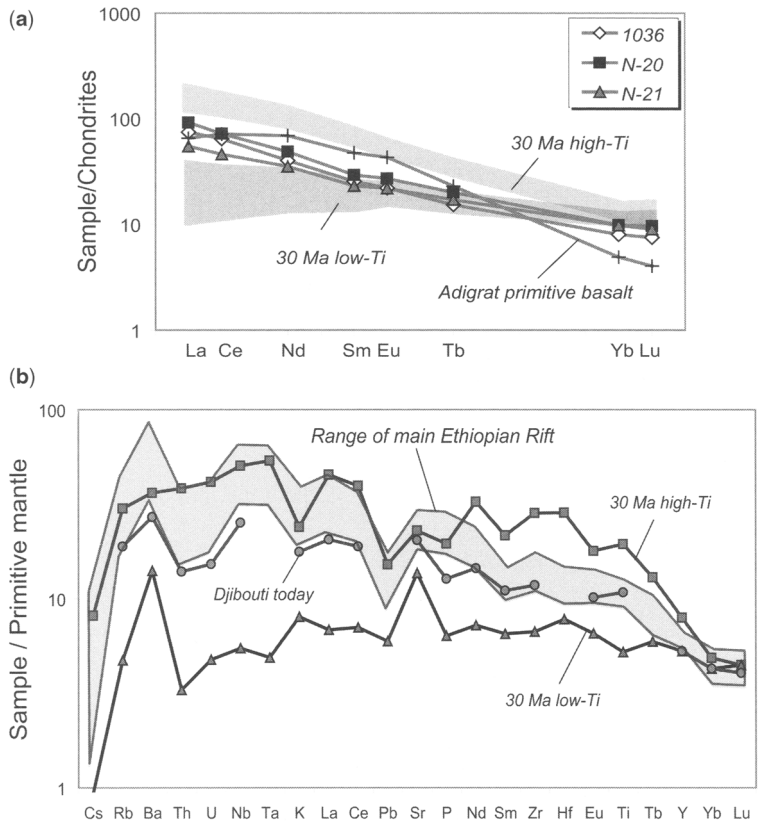

Fig. 3. Incompatible element abundances of selected Ethiopian lavas. (**a**) Rare earth elements. Modern rift basalts have abundances intermediate to those of low- and high-TiO_2 continental flood basalts (data from Pik *et al.* 1999; Kieffer *et al.* 2004); three representative samples are shown (see Table 1). A small number of primitive basalts from Adigrat have more highly concave REE patterns (Pik *et al.* 1999). Recent mafic lavas from Djibouti (Deniel *et al.* 1994) and 23 Ma Ethiopian basalts (Kieffer *et al.* 2004) have REE patterns (not shown) that fall within the range of the modern rift basalts (normalizing values of Boynton, 1984). (**b**) Primitive mantle-normalized incompatible trace element diagrams (normalizing values of Sun & McDonough 1989) for selected mafic lavas. The range of modern rift basalts is shaded; representative samples from Djibouti and the Oligocene low- and high-TiO_2 suites are shown for comparison. See text for discussion.

Dofan, the northernmost volcanic centre studied, have Sr–Nd–Pb isotope values that fall within the range of young plume-derived Djibouti and Erta 'Ale basalts (Fig. 5): $^{87}Sr/^{86}Sr \sim 0.7037$, $^{143}Nd/^{144}Nd \sim 0.51286$, $^{206}Pb/^{204}Pb \sim 18.83$, $^{208}Pb/^{204}Pb \sim 38.90$. Isotopic signatures trend slightly towards more enriched values from Dofan southward to Fantale and Kone. The most radiogenic values are seen at Boseti and Gedemsa, i.e. $^{87}Sr/^{86}Sr$ up to 0.7053. Post-rift basalts from the Addis Ababa series have isotopic compositions that overlap the Dofan lavas and extend to compositions similar to those observed at Fantale and Kone; syn-rift basalts sampled along the rift walls and away from the main rift axis have more enriched isotopic signatures similar to those at Boseti and Gedemsa.

At a regional scale, Sr–Nd isotope analyses do not allow individual source components to be distinguished reliably. Ethiopian rift basalts and the modern Afar plume both lie within the broad range defined by 30 million-year-old lavas from Ethiopia and Yemen; 23 Ma basalts from Choke and Guguftu plot within this field as well. The exceptions to this overall uniform picture are the two Oligocene high-Ti lavas from Adigrat noted previously to have unusual rare earth element abundances: these two samples have Sr–Nd isotopic compositions that are more depleted than any other Ethiopian lavas, and fall

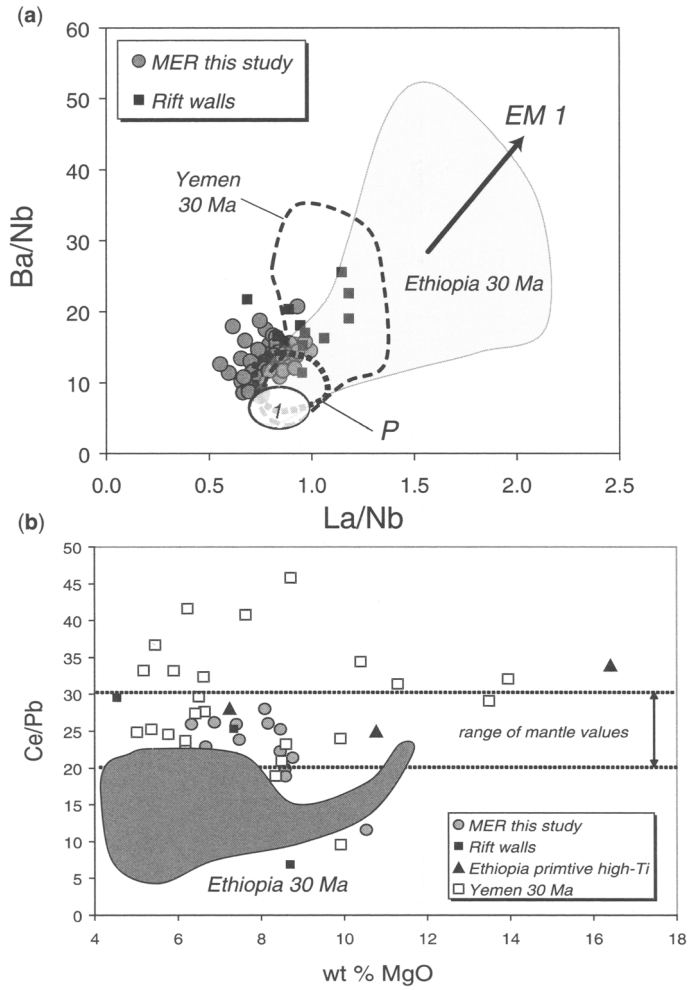

Fig. 4. Relative abundances of incompatible trace elements help constrain the source components that contribute to mafic volcanism. (**a**) La/Nb–Ba/Nb variations among modern rift basalts define a restricted range with La/Nb values similar to those of the primitive mantle, and Ba/Nb values somewhat elevated. Previously published analyses from the same region (Boccaletti *et al.* 1999, not shown) and our new data on syn-extensional basalts from the rift walls extend to higher values, requiring greater contributions from non-primitive source components. Most of the rift basalts plot near the field of young mafic lavas from Djibouti (Deniel *et al.* 1994) and Erta'Ale (Barrat *et al.* 1998), encircled by the dotted line and believed to represent the modern Afar plume. The Ethiopian (Pik *et al.* 1999; Kieffer *et al.* 2004) and Yemeni (Chazot & Bertrand 1993; Baker *et al.* 1996*a*) flood basalts define distinct ranges, but both groups are substantially enriched relative to the modern samples. The field labelled '1' encompasses primitive high-Ti Ethiopian lavas. (**b**) Ce/Pb–MgO variations show that most of the Main Ethiopian Rift lavas plot within the range of mantle-derived basalts, whereas the rift wall lavas and both Yemeni and Ethiopian flood basalts record contributions from lithospheric or crustal sources. Primitive high-Ti Ethiopian lavas plot within the range of mantle-derived basalts (sources of data: Baker *et al.* 1996*a*; Pik *et al.* 1999; Kieffer *et al.*).

near the MORB suite from the nearby West Sheba Ridge (Fig. 5).

Pb isotope signatures of the recent Ethiopian rift lavas form an array between the modern Afar plume and less radiogenic compositions broadly similar to those observed in 30-million-year-old continental flood basalts from both northern Ethiopia (including Adigrat) and Yemen (Fig. 5). These isotopic values are clearly distinct from compositions observed in Turkana, Kenya from 45 Ma through the present (Furman *et al.* 2004, 2006). Interestingly, the 23 Ma Ethiopian basalts from Choke and Guguftu with unusual major and trace element abundances have Pb isotopic

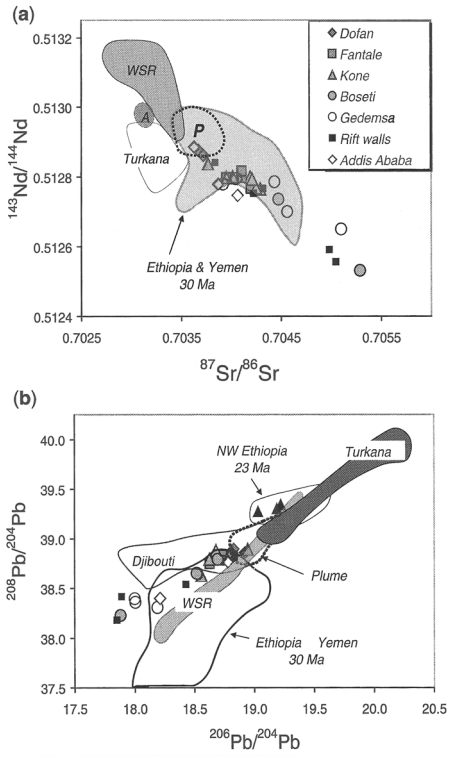

Fig. 5. Radiogenic isotope variations among Ethiopian lavas. (**a**) $^{87}Sr/^{86}Sr$–$^{143}Nd/^{144}Nd$ variations are strongly correlated among the recent rift lavas, and define a trend that extends from the Afar plume (labelled **P**), defined by mafic lavas from Djibouti (Deniel *et al.* 1994) and Erta' Ale (Barrat *et al.* 1998), towards radiogenic compositions more typical of crustal and lithospheric sources (Gedemsa data from Trua *et al.* 1999; Peccerillo *et al.* 2003). Lavas from Dofan, the northernmost volcano examined here, and the Addis Ababa series have isotopic compositions that overlap the Afar plume. Oligocene flood basalts (Chazot & Bertrand 1993; Baker *et al.* 1996*a*; Pik *et al.* 1999; Kieffer *et al.* 2004) define a broad range that encompasses many of the modern lavas but is distinct from Turkana basalts erupted 45 Ma through to the present (Furman *et al.* 2004, 2005). Two primitive high-Ti basalts from Adigrat (field labelled **A**) are compositionally distinct from all other basalts reported here. (**b**) The $^{206}Pb/^{204}Pb$–$^{208}Pb/^{204}Pb$ systematics of these sample suites further define the source components involved. Modern rift basalts vary from compositions overlapping the Afar plume to lower Pb isotope values, and generally overlap the range of 30 Ma flood basalts from both Ethiopia (including Adigrat) and Yemen. Lavas from Turkana have consistently higher Pb isotope compositions, ranging from a high-μ component sampled between 40–17 Ma to the modern Afar plume, and there is no overlap between the flood and rift basalts and the Turkana suite. Two 23 Ma lavas from Choke, Ethiopia (Kieffer *et al.* 2004) have elevated Pb isotope compositions relative to all other Ethiopian rocks (see text for discussion).

compositions that fall within the Turkana array rather than the long-term Ethiopia/Afar array (Fig. 5).

Discussion: melting histories and basaltic source regions

Depth and extent of melting

Modern Ethiopian rift basalts can be distinguished from the Oligocene continental flood basalts on the basis of major and trace element geochemistry, whilst the radiogenic isotopic compositions of the two groups show greater variability and, perhaps as a result, greater overlap. We first explore the extent to which the bulk geochemical differences reflect spatial and temporal variations in processes associated with melt extraction and emplacement, or whether they instead require distinct suites of lithospheric and sublithospheric source domains.

Primitive recent Ethiopian rift basalts have bulk compositions that can be derived by melting fertile spinel peridotite as suggested, for example, on the basis of their REE profiles (Fig. 3). The SiO_2 and FeO* contents of these lavas (back-corrected for olivine fractionation; Fig. 6) plot near the range of experimentally derived melts of fertile peridotite at a pressure of *c.* 30 kb (Baker & Stolper 1994; Kushiro 1996). The associated depth of *c.* 100 km is greater than the lithospheric thickness inferred on the basis of mantle tomography (e.g. Bastow *et al.* 2005; Tiberi *et al.* 2005). The melting pressures inferred for nepheline-normative lavas in this manner are slightly but consistently greater than those obtained for hypersthene-normative basalts (Fig. 6), although there is some overlap between the groups. A similar pattern is observed among young Djibouti lavas: samples with lower degrees of silica saturation indicate melting at greater depths than those inferred for hypersthene- and quartz-normative MgO-rich lavas (Fig. 6).

Among the Oligocene flood basalts, inferred pressures of melting range from 15 to $\geq$30 kb for hypersthene- and quartz-normative samples, and from 30 to >40 kb for nepheline-normative lavas. The more highly silica-saturated lavas also yield calculated primary melt compositions with higher SiO_2 and FeO* relative to the nepheline-normative lavas, consistent with their derivation by greater degrees of melting (cf. Kushiro 1996; Wasylenki *et al.* 2003). A more realistic picture of the melting process provides for polybaric melting, i.e. vertical aggregates of melts derived over a range of depths within a melting column that extends over tens of kilometres. The pressure

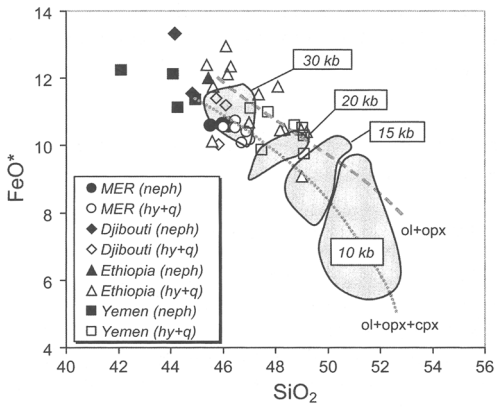

Fig. 6. FeO* versus SiO_2 for selected mafic lavas and experimental melts in equilibrium with mantle peridotite (Baker & Stolper 1994; Kushiro 1996). The dotted line connects experimental runs for melts coexisting with cpx + oliv + opx, and the dashed line connects experimental melts coexisting with oliv + opx after higher degrees of melt removal. Major element compositions were renormalized with total iron as FeO, then corrected for olivine fractionation to Mg# ~ 72; only samples with Mg# > 62 were corrected using this procedure. Experimental data are plotted as reported, and are shown in the enclosed fields. Filled symbols indicate calculated primary melts for lavas with nepheline-normative compositions; open symbols indicate starting compositions that are quartz- or hypersthene-normative. Calculated primary melts for nepheline-normative lavas indicate consistently higher pressures and lower extents of melting than the more silica-saturated compositions. Sources of data: Deniel *et al.* 1994; Baker *et al.* 1996*a*; Pik *et al.* 1999; Kieffer *et al.* 2004.

estimates presented here provide simply a framework for comparison. Interestingly, there is no geographical control on the calculated melting depths, as lavas from Ethiopia and Yemen indicate comparable melting conditions. Most of the low-Ti Oligocene lavas are too evolved to be evaluated using this calculation scheme, as they have MgO contents below 7 wt.% and have undergone extensive fractionation of olivine ± clinopyroxene ± plagioclase feldspar (Pik *et al.* 1998, 1999).

Identifying lithospheric and sub-lithospheric source regions

Prior studies of the Ethiopia–Yemen continental flood basalts and Plio-Quaternary lavas from the Afar region have identified several distinct source domains that contribute to magma genesis. To first order, these components include the Afar plume, one or more additional mantle reservoir(s), and a subordinate contribution from the continental crust or mantle lithosphere (Hart *et al.* 1984; Chazot & Bertrand 1993; Baker *et al.* 1996*a*, 2000; Pik *et al.* 1999; Kieffer *et al.* 2004). The Afar plume is broadly thought to include a component with $^{87}Sr/^{86}Sr$ ~0.704, $^{143}Nd/^{144}Nd$ ~0.51295, $^{206}Pb/^{204}Pb$ ~18.8 and $^{3}He/^{4}He$ up to 19 R/R_A (Hart *et al.* 1989; Schilling *et al.* 1992; Vidal *et al.* 1991; Marty *et al.* 1993, 1996; Deniel *et al.* 1994; Scarsi & Craig 1996; Pik *et al.* 1999), but the compositions of the remaining source regions are poorly constrained. For example, Hart *et al.* (1989) infer an enriched mantle component, while Pik *et al.* (1999) infer the presence of both MORB-like mantle and a second depleted component.

One reason for the lack of consensus is that Pb isotope compositions vary widely among Ethiopian plateau and rift lavas, and tend not to correlate well with Sr–Nd systematics (Fig. 5). Although Pb isotopic compositions of mafic melts are often heterogeneous at all scales, presumably reflecting melt segregation and aggregation processes (Saal *et al.* 1998; Kent *et al.* 2002; Bryce & DePaolo 2004), there are consistent spatial and temporal patterns among the lavas that correlate with both geographical and geochemical parameters, bringing us closer to an integrated understanding of the source regions.

Following Hart (1984), we use the dimensionless parameter $\Delta 8/4$ to systematize variations in Pb isotopic composition ($\Delta 8/4$ indicates the difference in $^{208}Pb/^{204}Pb$ of a sample relative to the Northern Hemisphere Reference Line; see Table 1); this parameter itself has no physical meaning but provides a framework within which to evaluate chemical distinctions among and between sample suites. Variations in $\Delta 8/4$- $^{87}Sr/^{86}Sr$ among the flood basalts and recent mafic lavas show clear regional trends that can be interpreted in terms of source regions sampled by the melting process (Fig. 7; Baker *et al.* 1996*a*). The modern Afar plume is well-constrained by the isotopic compositions of MgO-rich lavas from Erta 'Ale and Djibouti, and the remaining samples form linear arrays that radiate from this region of isotopic space.

Recent lavas from the Ethiopian rift and Djibouti define a trend towards high, EM1-like $^{87}Sr/^{86}Sr$ and $\Delta 8/4$. Samples in this group have La/Nb-Ba/Nb values that are not dramatically elevated relative to primitive mantle, so they indicate a radiogenic source region with only moderately enriched incompatible trace element abundances, interpreted as the lower crust (Baker *et al.* 1996*a*; Trua *et al.* 1999). A second well-defined trend among flood basalts from Ethiopia and Yemen extends towards high, EMII-like $^{87}Sr/^{86}Sr$ and low $\Delta 8/4$ values. This trend was interpreted by Baker *et al.* (1996a) as indicating an upper crustal component. The

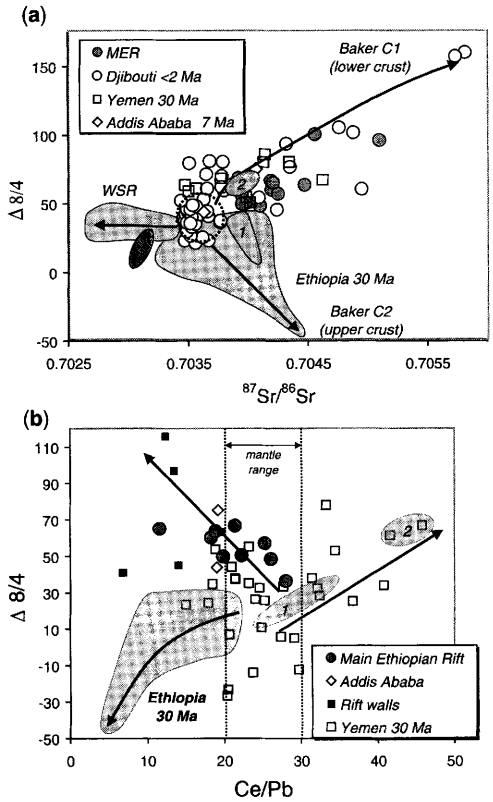

Fig. 7. $^{87}Sr/^{86}Sr$ and Ce/Pb vs. Δ8/4 require regional and temporal differences in source components contributing to mafic volcanism in the Afar region. Prior to plotting, samples from Yemen where crustal contamination could be demonstrated through anomalously high values of $^{207}Pb/^{204}Pb$ and/or $\delta^{18}O$ (Baker *et al.* 1996*a*, 2000) were removed. (**a**) Regional sample suites define tight arrays that extend from the Afar plume (dotted circle; data from Djibouti (Deniel *et al.* 1994) and Erta' Ale (Barrat *et al.* 1998) towards distinct additional source regions. Labelled components from Baker *et al.* (1996*a*) are discussed in the text. Fields labelled 1 and 2 indicate primitive high-Ti Oligocene lavas from Ethiopia (Pik *et al.* 1999) and Yemen (Baker *et al.* 1996a), respectively; field 3 encircles primitive Oligocene Adigrat basalts (Pik *et al.* 1999). Data on mid-ocean basalts from the nearby West Sheba Ridge (WSR) are from Schilling *et al.* (1992); Main Ethiopian Rift (MER) samples include lavas in Table 1 and data from Trua *et al.* (1999) and Peccarillo *et al.* (2003). (**b**) High Δ8/4 components recorded in young Main Ethiopian Rift (MER) lavas and Oligocene Yemen continental flood basalts (Baker *et al.* 1996*a*) can be resolved by their distinct Ce/Pb values. These data indicate distinct source components in each region that lie outside the range of mantle-derived liquids (Hofmann *et al.* 1996). All samples plotted here have >6.5 wt% MgO. Fields labelled 1 and 2 indicate primitive high-Ti Oligocene lavas from Ethiopia (Pik *et al.* 1999) and Yemen (Baker *et al.* 1996*a*), respectively. See text for discussion.

high Ba/Nb–La/Nb values of these samples suggest instead that the high $^{87}Sr/^{86}Sr$ component may reside in the enriched mantle lithosphere; low degrees of melting can also produce variations in these parameters, but the quartz- and hypersthene-normative compositions of these lavas are not consistent with low degrees of mantle melting. There is evidence that the source region was metasomatized to a small degree by hydrous fluids: the high Ba and low K contents of the lavas relative to Kone basalts suggest the presence of amphibole. Interestingly, the primitive high-Ti lavas interpreted by Pik *et al.* (1999) as representing the essential Oligocene plume (HT2 series) also plot within this array, suggesting they include a contribution from hydrated mantle lithosphere. The high degrees of melting inferred for both of these sample groups makes assimilation of surrounding lithologies during ascent physically plausible.

The third distinct trend observed among the mafic lavas examined here is defined by recent sea-floor basalts from the West Sheba Ridge near Djibouti (Schilling *et al.* 1992). These samples define an array trending from the modern plume composition towards lower $^{87}Sr/^{86}Sr$ at near-constant Δ8/4. We interpret this trend to indicate involvement of the convecting upper-mantle source region for mid-ocean ridge basalts. Note that the high-Ti lavas from Adigrat plot along this array and are clearly isotopically different from all other lavas observed in the Oligocene through Recent Ethiopian volcanic provinces. We emphasize that the volume of these lavas is small, and their occurrence rare, but they provide insight into a source component apparently sampled only during flood basalt volcanism.

To resolve the additional components involved in long-term Afar volcanism we incorporate trace element evidence, as relative abundances of incompatible trace elements are sensitive to the mineralogy of specific source regions. Variations in Ce/Pb against Δ8/4 (Fig. 7) show clearly the trend of crustal involvement for Ethiopian Oligocene basalts identified above. Interestingly, trends for modern Ethiopian rift lavas and Oligocene Yemen flood basalts can be distinguished from one another on the basis of their distinct Ce/Pb values. From this diagram, we conclude that the crustal source sampled by the modern Ethiopian rift lavas has been available throughout development of the rift, whereas the Yemen rocks record involvement of a separate crustal component that is absent in Ethiopia.

We can also combine our understanding of the melting conditions with the isotopic characteristics of the basalts. In each area, basalts derived at higher pressures and/or through lower degrees of melting

(i.e. nepheline-normative compositions) have more depleted Sr and Nd isotopic signatures than corresponding lavas that are derived at more shallow depths and/or through greater extents of melting (Fig. 8). This observation reinforces the existence of an extended melting column within the mantle, and helps constrain the occurrence of different source domains in space and time.

The integrated geochemical evidence allows us to identify the source components involved in regional volcanism over the past 30 million years. First, Oligocene through Recent basalt volcanism in Ethiopia, Yemen and Djibouti includes a contribution from a common composition which we interpret as the Afar plume (Fig. 8). This component is identifiable on the basis of Sr–Nd–Pb isotopes and incompatible trace element abundances in basalts of all ages from throughout the region (Figs 4 and 5). Its persistence through time suggests that it forms the core of the upwelling mantle plume, and its occurrence in melts formed at high pressures indicates that it is a fertile composition. This plume composition appears to be nearly constant in both space and time, and that all of the regional trace element and isotopic data form binary arrays that radiate from this composition towards geochemically distinct end-members (cf. Schilling *et al.* 1992).

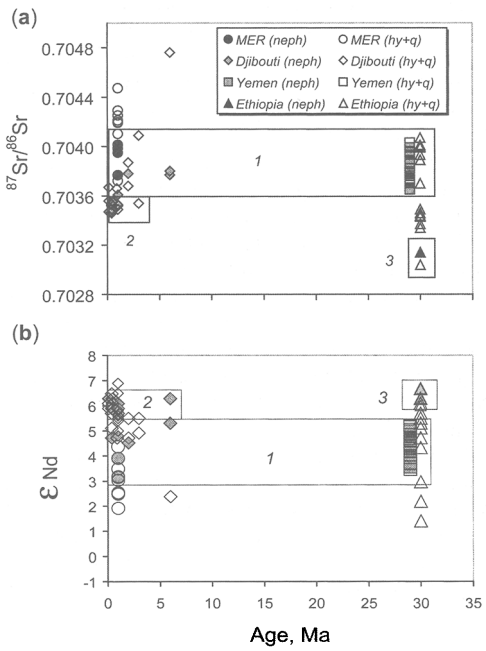

Fig. 8. Temporal and spatial variations in Sr–Nd isotopic compositions of primitive (>6.5 wt% MgO) lavas from Ethiopia, Yemen and the modern Afar plume indicate three source components present at low degrees of mantle melting. Each of these source components is isotopically unradiogenic relative to those recorded in lavas derived by higher degrees of melting. Box 1 encompasses a compositional range similar to bulk silicate earth that is found in lavas of all ages, interpreted here as representing the core of the Afar plume. Box 2 is a MORB-like composition found in ocean floor basalts and lavas from Djibouti (Deniel *et al.* 1994) and Erta' Ale (Barrat *et al.* 1998). Box 3 encloses lavas from Adigrat, Ethiopia (Pik *et al.* 1999). See text for discussion.

Three compositionally distinct source domains can be identified on the basis of the mixing trajectories. One is the depleted mantle (DMM), observed both in recent lavas from Djibouti and Erta 'Ale and in primitive Oligocene lavas from Adigrat, Ethiopia (Fig. 8). We also identify an enriched mantle (EMI-like) or crustal component in both low- and high-Ti mafic lavas from the entire Ethiopian plateau; these lavas are characterized by higher La/Nb–Ba/Nb values and require higher time-integrated parent–daughter ratios to account for their more radiogenic isotope compositions relative to the plume or DMM. A second enriched component (EMII-like) is recorded in within-rift and rift wall basalts from central Ethiopia and Djibouti, the off-rift volcanics from the Addis Ababa series, and the Oligocene Yemen basalts. We concur with Baker *et al.* (1996*a*) and Trua *et al.* (1999) that this source is located in the lower crust; alternatively the enriched source may represent mafic magmas emplaced during the earliest stage of flood basalt activity (e.g. Mackenzie *et al.* 2005; Maguire *et al.* 2006).

Two observations about the enriched source domains and their occurrence are significant. First, the enriched mantle contributions are found only in lavas derived from moderate degrees of mantle melting. Secondly, each enriched mantle composition forms a unique mixing array with the Afar plume. Together, these observations indicate that the plume records melting of chemically distinct source domains in the lithosphere and asthenosphere. This conclusion is consistent with numerical models that suggest an ascending plume will melt or displace, rather than entrain, surrounding and overlying mantle material (Farnetani *et al.* 2002).

Geodynamic evolution of the region

Documenting the head-to-tail transition

Numerical modelling of thermochemical plumes derived from a deep mantle thermal boundary layer predicts that geochemical domains present within a plume head will also be preserved in magmatism associated with the plume tail (Farnetani *et al.*

2002). This prediction results in part from the observation that ascending plume material displaces, rather than entrains, surrounding ambient upper mantle, so heterogeneities are thinned and stretched, preserving discrete flow paths within the plume core. We use this numerical prediction, derived for vigorous plumes emplaced beneath oceanic lithosphere, as a framework to assess geochemical heterogeneity in mafic lavas derived from the Afar plume throughout its 30 million-year history. Long-lived spatial variability in plume tails has been documented in Hawaii (e.g. Lassiter & Hauri 1998; DePaolo *et al.* 2001; Blichert-Toft *et al.* 2003; Mukhopadhyay *et al.* 2003; Kurz *et al.* 2004; Abouachami *et al.* 2005; Bryce *et al.* 2005) and the Galápagos (Geist 1992; White *et al.* 1993; Hoernle *et al.* 2000; Harpp & White 2001; Geldmacher *et al.* 2003; Thompson *et al.* 2004). There are good reasons to expect that the results from Afar may differ from those observed in the oceanic setting: the Afar plume has a substantially lower buoyancy flux than those calculated for Hawaii, Galápagos and Iceland (Ebinger & Sleep 1998) and was emplaced beneath thick continental lithosphere. In addition, the sampling density in the Ethiopia–Yemen flood basalt province is not yet sufficient to resolve consistent spatial variations in lava chemistry. Nonetheless, our results will help test the robustness of the numerical models developed for oceanic hot spots.

The new data presented here indicate temporal trends in source availability and mixing that in turn provide insight into the long-term evolution of the Afar plume system. The Oligocene flood basalts in Ethiopia form the thickest sequence, indicating the highest flux of both material and heat. Significantly, these lavas show the greatest and most uniform contribution from the lithospheric mantle, indicating high degrees of melting over a broad region. This lithospheric source region apparently does not play a major role in generating the recent MER basalts, suggesting it has been thinned and/or partially removed under the rift axis itself. In contrast, lithospheric geochemical signatures dominate the chemistry of lavas from highly extended portions of southwestern Ethiopia (Stewart & Rogers 1996; George *et al.* 1998; Rogers *et al.* 2000) and much of the Kenya rift (e.g. Macdonald 1994; Späth *et al.* 2001), indicating that lithospheric removal is not widespread.

The geochemical evidence suggests that the total magmatic and thermal flux of the Afar plume has waned through time. Modern mafic lavas from Djibouti, Erta' Ale and the Main Ethiopian Rift often show evidence of crustal interaction, presumably occurring in magma chambers within the crust (e.g. Ayalew *et al.* 2006). In the modern rift, low magma supply rates over the past 3 million years led to development of nested silicic calderas at, for example, Kone and Gedemsa. We suspect that the low magma flux calculated for the modern Afar plume relative to Hawaii and the Galápagos (Ebinger & Sleep 1998) means that it may not be feasible to correlate quantitatively any spatial variations in the chemical domains over the life of the Afar plume.

Geochemical evidence for one- and two-plume models

The recognition of long-lived geochemically consistent contributions to magmatism in the Ethiopia–Yemen region supports models that call upon the Afar plume to be the source for both Oligocene (plume head) and recent (plume tail) magmatism. The broad distribution of long-lived volcanism in Ethiopia and portions of the East African rift has led to various models of plume structure. The suggestion that there are two discrete plumes (George *et al.* 1998; Rogers *et al.* 2000) was based on Sr–Nd isotopic compositions of lavas from southern Ethiopia and the Kenya rift. Although appealing in some ways, this model has two difficulties that have not been overcome: (1) it does not adequately account for the distribution of lavas within the EARS, as no viable plume track exists for the proposed Kenya plume; and (2) the south Ethiopian lavas were primarily derived from the lithosphere and thus provide little insight into sub-lithospheric processes (Furman *et al.* 2004).

The single-plume model proposed by Ebinger & Sleep (1998) places a plume head beneath southern Ethiopia at *c.* 45 Ma and attributes widespread Cenozoic magmatism (e.g. Hoggar and Tibesti massifs, the modern Afar area) to the lateral transport of plume material along zones of thinned lithosphere. This model benefits from physical simplicity, but is not immediately consistent with recent geophysical studies indicating possible plume stems beneath both Afar and the Tanzania craton (Debayle *et al.* 2001; Nyblade *et al.* 2000; Weeraratne *et al.* 2003; Montelli *et al.* 2004).

Similarly, the consistent Pb isotope differences between contemporaneous sub-lithospheric magmas erupted in Ethiopia and Turkana (Furman *et al.* 2004, 2005) are compatible with the geophysical evidence for separate plume stems beneath these two areas. Turkana lavas have a distinctive high $^{206}Pb/^{204}Pb$ signature that is not observed in mafic lavas associated with the Afar plume. This characteristic Pb isotopic signature is, however, found in other areas associated with the South African superplume (e.g. St Helena – Chaffey *et al.* 1989; South Africa – Janney *et al.* 2002). Over the long history of volcanism in Ethiopia

and Turkana, only basalts from the 23 Ma Choke shield volcano have Pb isotope compositions that plot within the Turkana array (Fig. 5; Kieffer *et al.* 2004). These data are intriguing because they may indicate northward magma transport associated with volcano-tectonic activity at 23 Ma in the Turkana area (Furman *et al.* 2006).

The isotopic data thus cannot discriminate between models invoking two unrelated plumes (e.g. George *et al.* 1998) or one large heterogeneous plume with multiple stems as predicted by numerical and experimental results (Ishida *et al.* 1999; Davaille *et al.* 2003). The clear geophysical evidence for the South African superplume (Ritsema *et al.* 1999; Gurnis *et al.* 2000; Zhao 2001; Ni *et al.* 2002) appears to favour the latter scenario, although the shallow mantle structure cannot yet be resolved in sufficient spatial detail. The two small isotopically distinct plume stems may rise from the superplume and interact with regionally unique crustal and sublithospheric sources during ascent. Tomographic investigation of plume pairs (Azores and Canaries, Ascension and St Helena) indicates that two areas of upwelling can merge at mantle depths over 1000 km, thus tapping a common source at depth (Montelli *et al.* 2004). The large physical dimension of the South African superplume—it represents the largest-known heat and mass transfer from the lowermost portion of the mantle (e.g. Romanowicz & Gung 2002) — makes it likely that a variety of source materials coexist within the ascending region, and hence two or more chemically distinct plume heads could come from the same major deep mantle thermal and chemical anomaly.

Conclusions

Mafic lavas from Ethiopia and Yemen record 30 million years of volcanism associated with the Afar plume. Modern Ethiopian rift basalts have major and trace element geochemical features that are distinct from those of the Oligocene continental flood basalts, whereas the isotopic characteristics of these groups show greater overlap. The geochemical differences can be interpreted in terms of melting processes (depth and degree of melting), as well as mixing of melts of the Afar plume and from mantle sources with three end-member compositions. Taken together, the geochemical evidence indicates that the Afar plume is a long-lived feature of the mantle and that its fundamental isotopic composition has effectively not changed during the transition from Oligocene plume head volcanism to modern plume tail activity. Temporal changes in Ethiopian volcanic geochemistry thus appear to reflect the evolving tectonic environment rather than a significant change in sub-lithospheric source composition.

Specifically, we find that:

1. Oligocene lavas are generally derived by greater degrees of melting than the recent basalts. Most of the flood basalts are hypersthene- and quartz-normative, while the younger lavas include a higher proportion of nepheline-normative compositions.

2. The isotopic compositions of Ethiopian and Yemeni basalts of all ages are linked with the depth and degree of melting: the Sr and Nd isotopic signatures of lavas derived from smaller degrees of melting and/or melting at higher pressure are more depleted than those signatures found in lavas derived at shallower depths and/or through greater extents of melting.

3. The Sr- and Pb-isotopic signatures of Oligocene through Recent mafic lavas define three distinct binary mixing arrays that radiate from a common composition interpreted as the Afar plume. The end-members involved in mixing include both depleted (DM, interpreted as the convecting upper mantle source region for mid-ocean ridge basalts) and enriched (EMI-like, inferred to be within the lower crust and EMII-like, inferred to reside within the upper crust) mantle components, each of which is observed in a geographically restricted area.

4. Lack of ternary mixing among these components suggests that the ascending plume melts chemically distinct local source domains in the overlying asthenosphere and lithosphere, rather than entraining and incorporating ambient mantle on a regional scale.

This research was funded by NSF-EAR 0207764 and a George H. Deike, Jr. grant from The Pennsylvania State University to T. Furman. J. Bryce acknowledges support from NSF-EAR 0338385 during preparation of the manuscript. We are grateful to E. Klein and G. Dwyer for performing major and trace element analyses. Special thanks to Kassahun Ejeta and Roeland Doust for masterful assistance during field work. Thanks also to Daniel and Elizabeth Larson for help with sampling and field logistics. We gratefully acknowledge the many thought-provoking conversations with members of EAGLE-US, UK and Ethiopia throughout this project. The manuscript benefited greatly from thoughtful reviews by G. WoldeGabriel and R. Macdonald; we thank C. Ebinger for careful editorial handling.

Appendix

Supplemental material: analytical procedures

E99- and KO-series lavas and samples AA99-6, -19 were analysed at the Centre Récherches

Pétrographiques et Géochimiques, Nancy, France by G. Yirgu (major elements by ICP-AES and trace elements by ICP-MS). All other lavas were analysed for major and minor elements (including Ba and Sr) by DCP on an ARL-Fisons Spectraspan 7 and for P_2O_5 and all trace elements by ICP-MS using a VG PlasmaQuad-3 at Duke University (M. Rudnicki and G. Dwyer, analysts). Precision based on replicate analyses of samples and natural basalt standards are generally $<1\%$ for SiO_2, Sr, Y, Zr, Nb, La, Ce; $<3\%$ for other major elements, Ba, Sr, Rb, Cs, Cr, Sc, V, Co, Pr, Nd, Sm, Eu, Gd, Tb, Dy, Ho, Er, Hf and Ta; $<5\%$ Ni, Yb, Lu, Pb, Th and $<8\%$ for U. All oxides are presented as wt %; trace elements are given as ppm.

All Pb analyses, a majority of the Nd analyses, and several Sr analyses were carried out in the clean laboratories and analytical facilities at San Diego State University. These Sr, Nd, and Pb isotope ratios were determined from a single HF-HNO_3 dissolution of approximately 0.4 g of rock powder. Pb was separated according to a two-column anion exchange chromatographic procedure described by Hanan & Schilling (1989). Nd and Sr elemental concentrations were subsequently carried out using procedures modified from Schilling *et al.* (1994), with Eichrom Ln-Spec resin for the rare earth separation, and Eichrom Sr-Spec as a final step for cleaning up the Sr. The total analytical blanks for these procedures were <90 pg Pb, <200 pg Nd, and <300 pg Sr. Thus no blank corrections were made to the data reported in Table 1. At SDSU, the Nd and Pb isotope ratios were measured on the Nu Plasma HR by multicollector inductively coupled plasma mass spectrometry (MC-ICP-MS). Sr isotope ratios were measured using VG Instruments Sector 54 seven-collector thermal ionization mass spectrometer. The $^{143}Nd/^{144}Nd$ and $^{87}Sr/^{86}Sr$ ratios were normalized to correct for mass fractionation using values of $^{146}Nd/^{144}Nd = 0.7219$ and $^{88}Sr/^{86}Sr = 0.1194$, respectively. The $^{143}Nd/^{144}Nd$ of AMES Nd standard $= 0.512\,118 \pm 0.000\,003$, and the NIST SRM 987 Sr standard $= 0.710\,219 \pm 0.000\,005$ (all $2\sigma/n$). Sr isotopic data in Table 1 are renormalized to NIST SRM $987 = 0.710\,250$. The Nd reported in Table 1 is given relative to La Jolla Nd $= 0.511\,816$. Pb isotope compositions analysed by MC-ICP-MS on the Nu Plasma HR at SDSU using the Tl-doping technique with NIST SRM 997 Tl and $^{205}Tl/^{203}Tl = 2.3889$ (White *et al.* 2000; Thirlwall 2002; Albarède *et al.* 2004). NIST SRM981 was used to correct the Pb isotope data for fractionation and machine bias (White *et al.* 2000). The NIST 981 standard was run every second or third analysis. The final Pb data were adjusted to the Todt *et al.* (1996) values for NIST 981 relative to the bracketing standard runs. The NIST SRM 981 Pb standard averaged (with $2\sigma/n$) $^{206}Pb/^{204}Pb = 16.9372$ (0.0006), $^{207}Pb/^{204}Pb = 15.4915$ (0.0006), and $^{208}Pb/^{204}Pb = 36.6957$ (0.0016) during the analysis period. The uncertainties for the Pb isotope ratios, representing error propagation of the in-run $2\sigma/n$ analytical errors plus the $2\sigma/n$ reproducibility of the standards, were less than 0.002 for $^{206}Pb/^{204}Pb$ and $^{207}Pb/^{204}Pb$ and <0.006 for $^{208}Pb/^{204}Pb$.

A portion of the Sr and Nd isotopic measurements presented in Table 1 were carried out in the W. M. Keck Foundation Center for Isotope Geochemistry at UCLA. Approximately 200–250 mg aliquots of whole rock powders were digested in a HF–HNO_3 mixture. Samples for Sr isotopic study were prepared using standard ion chromatographic separation techniques employing cation exchange resins. Rare earth separations were carried out using a procedure involving a second cation ion exchange resin. Purified Sr salts were loaded in Ta_2O_5 on rhenium filaments for analysis. The strontium isotopic measurements were made via thermal ionization mass spectrometry (TIMS) on a VG sector-54 multicollector mass spectrometer operating in dynamic mode. Isotopic fractionation was corrected with an internal normalization of $^{86}Sr/^{88}Sr = 0.1194$. The average for NIST SRM 987 measured during the course of these analyses was $0.710\,238 \pm 0.000\,027$ (2σ). The $^{87}Sr/^{86}Sr$ values reported in Table 1 are normalized to NBS-987 values of 0.710 250. Neodymium isotopic measurements were also carried out TIMS on a Sector 54-30 multicollector operating in dynamic mode; Nd isotopic compositions were normalized to $^{146}Nd/^{144}Nd = 0.7219$ to correct for within-run fractionation. Standards run over the course of the analyses provided mean values (with 2σ) of the La Jolla standard ($n = 5$) of $^{143}Nd/^{144}Nd = 0.511\,830 \pm 0.000\,017$ (2σ). Two replicate samples were measured for Nd isotopic compositions in both the UCLA and SDSU facilities. These samples (N22 and E43) agreed in $^{143}Nd/^{144}Nd$ values within 0.000 022, or well within the overlapping uncertainties. The values reported in the table for these two samples are those evaluated at SDSU. For the sake of consistency, the UCLA Nd isotopic data are normalized to the SDSU values for the La Jolla Nd standard (i.e. $^{143}Nd/^{144}Nd = 0.511\,816$).

References

ABOUACHAMI, W., HOFMANN, A.W., GALER, S.J.G., FREY, F.A., EISELE, J. & FEIGENSON, M. 2005. Lead isotopes reveal bilateral asymmetry and vertical continuity in the Hawaiian mantle plume. *Nature*, **434**, 851–856.

ALBARÈDE, F., TÉLOUK, P., BLICHERT-TOFT, J., BOYET, M., AGRANIER, A. & NELSON, B. 2004. Precise and accurate isotopic measurements using multiple-collector ICPMS. *Geochimica et Cosmochimica Acta*, **68**, 2725–2744.

ARNDT, N.T., CZAMANSKE, G.K., WOODEN, J.L. & FEDORENKO, V.A. 1993. Mantle and crustal contributions to continental flood volcanism. *Tectonophysics*, **223**, 39–52.

AYALEW, D., EBINGER, C., BOURDON, E., WOLFENDEN, E., YIRGU, G. & GRASSINEAU, N. 2006. Temporal compositional variation of early syn-rift rhyolites along the southwestern Red Sea and northern Main Ethiopian Rift: implications for dyking of the crust. *In*: YIRGU, G., EBINGER, C.J. & MAGUIRE, P.K.H. (eds) *The Afar Volcanic Province within the East African Rift System*. Geological Society, London, Special Publications, **259**, 121–130.

BAKER, J.A., THIRLWALL, M.F. & MENZIES, M.A. 1996*a*. Sr–Nd–Pb isotopic and trace element evidence for crustal contamination of plume-derived flood basalts: Oligocene flood volcanism in western Yemen. *Geochimica et Cosmochimica Acta*, **60**, 2559–2581.

BAKER, J.A., SNEE, L. & MENZIES, M. 1996*b*. A brief Oligocene period of flood volcanism in Yemen: implications for the duration and rate of continental flood volcanism at the Afro-Arabian triple junction. *Earth and Planetary Science Letters*, **138**, 39–55.

BAKER, J.A., MACPHERSON, C.G., MENZIES, M.A., THIRLWALL, M.F., AL-KADASI, M. & MATTERY, D.P. 2000. Resolving crustal and mantle contributions to continental flood volcanism, Yemen; constraints from mineral oxygen isotope data. *Journal of Petrology*, **41**, 1805–1820.

BAKER, M.B. & STOLPER, E.M. 1994. Determining the composition of high-pressure mantle melts using diamond aggregates. *Geochimica et Cosmochimica Acta*, **58**, 2811–2827.

BARRAT, J.A., FOURCADE, S., JAHN, B.M., CHEMINÉE, J.L. & CAPDEVILA, R. 1998. Isotope (Sr, Nd, Pb, O) and trace element geochemistry of volcanics from the Erta' Ale range (Ethiopia). *Journal of Volcanology and Geothermal Research*, **80**, 85–100.

BASTOW, I.D., STUART, G.W., KENDALL, J.-M. & EBINGER, C.J., 2005. Upper-mantle seismic structure in a region of incipient continental breakup: northern Ethiopian Rift. *Geophysical Journal International*, **162**, 479–493.

BENOIT, M., NYBLADE, A., TUJI, M., AYELE, A., ASFAW, L., LANGSTON, C. & VANDECAR, J. 2003. Upper mantle seismic velocity structure beneath East Africa and the depth extent of thermal anomalies. *Geophysical Research Abstracts*, **5**, 07361.

BERTRAND, H., CHAZOT, G., BLICHERT-TOFT, J. & THORAL, S. 2003. Implications of widespread high-μ volcanism on the Arabian Plate for Afar mantle plume and lithosphere composition. *Chemical Geology*, **198**, 47–61.

BLICHERT-TOFT, J., FREY, F.A. & ALBARÈDE, F. 1999. Hf isotope evidence for pelagic sediments in the source of Hawaiian basalts. *Science*, **285**, 879–882.

BLICHERT-TOFT, J., WEIS, D., MAERSCHALK, C., AGRANIER, A. & ALBARÈDE, F. 2003. Hawaiian hot spot dynamics as inferred from the Hf and Pb isotope evolution of Manua Kea volcano. *Geochemistry, Geophysics, Geosystems*, **4**, 8704, doi:10.1029/2002GC000340, 2003.

BOCCALETTI, M., MAZZUOLI, R., BONINI, M., TRUA, T. & ABEBE, B. 1999. Plio-Quaternary volcanotectonic activity in the northern sector of the Main Ethiopian Rift: relationships with oblique rifting. *Journal of African Earth Sciences*, **29**, 679–698.

BRYCE, J.G. & DEPAOLO, D.J. 2004. Pb isotopic heterogeneity in basaltic phenocrysts. *Geochimica et Cosmochimica Acta*, **68**, 4453–4468.

BRYCE, J.G., DEPAOLO, D.J. & LASSITER, J.C. 2005. Geochemical structure of the Hawaiian plume: Sr, Nd, and Os isotopes in the 2.8 km HSDP-2 section of Mauna Kea volcano. *Geochemistry, Geophysics, Geosystems*, **6**, Q09G18, doi: 10.1029/2004GC000809.

BURKE, K. 1996. The African plate. *South African Journal of Geology*, **99**, 339–409.

CALAIS, E., EBINGER, C., HARTNADY, C. & NOCQUET, J.M. 2006. Kinematics of the East African Rift from GPS and earthquake slip vector data. *In*: YIRGU, G., EBINGER, C.J. & MAGUIRE, P.K.H. (eds) *The Afar Volcanic Province within the East African Rift System*. Geological Society, London, Special Publications, **259**, 9–22.

CHAFFEY, D.J., CLIFF, R.A. & WILSON, B.M. 1989. Characterization of the St. Helena magma source. *In*: SAUNDERS, A.D. & NORRY, M.J. (eds) *Magmatism in the Ocean Basins*. Geological Society, London, Special Publications, **42**, 257–276.

CHAZOT, G. & BERTRAND, H. 1993. Mantle sources and magma-continental crust interactions during early Red Sea–Gulf of Aden rifting in Southern Yemen; elemental and Sr, Nd, Pb isotope evidence. *Journal of Geophysical Research*, **98**, 1819–1835.

CHERNET, T. & HART, W.K. 1999. Petrology and geochemistry of volcanism in the northern Main Ethiopian Rift–southern Afar transition region. *Acta Vulcanologica*, **11**, 21–41.

DAVAILLE, A., LE BARS, M. & CARBONNE, C. 2003. Thermal convection in a heterogeneous mantle. *Comptes Rendus Geoscience*, **335**, 141–156.

DAVIDSON, A. & REX, D.C. 1980. Age of volcanism and rifting in southwestern Ethiopia. *Nature*, **283**, 657–658.

DEBAYLE, E., LEVEQUE, J.-J. & CARA, M. 2001. Seismic evidence for a deeply rooted low-velocity anomaly in the upper mantle beneath the northeastern Afro/Arabian continent. *Earth and Planetary Science Letters*, **193**, 423–436.

DENIEL, C., VIDAL, P., COULON, C., VELLUTINI, P.-J. & PIGUET, P. 1994. Temporal evolution of mantle sources during continental rifting: the volcanism of Djibouti. *Journal of Geophysical Research*, **99**, 2853–2869.

DEPAOLO, D.J., BRYCE, J.G., DODSON, A., SHUSTER, D. & KENNEDY, B. 2001. Isotopic evolution of Mauna Loa and the chemical structure of the Hawaiian

plume. *Geochemistry, Geophysics, Geosystems*, **2**(7), doi:10.1029/2000GC000133.

DUGDA, M.T., NYBLADE, A.A., JULIA, J., LANGSTON, C.A., AMMON, C.J. & SIMIYU, S. 2005. Crustal structure in Ethiopia and Kenya from receiver function analysis. *Journal of Geophysical Research*, **110**, B01303.

DUNCAN, R.A. 1981. Hotspots in the southern ocean—An absolute framework of reference for motion of the Gondwana continents, *Tectonophysics*, **74**, 29–42.

EWART, A., MARSH, J.S., MILNER, S.C., DUNCAN, A.R., KAMBER, B.S. & ARMSTRONG, R.A. 2004. Petrology and geochemistry of Early Cretaceous bimodal continental flood volcanism of the NW Etendeka, Namibia; Part 1, Introduction, mafic lavas and re-evaluation of mantle source components. *Journal of Petrology*, **45**, 59–105.

EBINGER C.J. & SLEEP N.H. 1998. Cenozoic magmatism throughout east Africa resulting from impact of a single plume. *Nature*, **395**, 788–791.

FARNETANI, C.G., LEGRAS, B. & TACKLEY, P.J. 2002. Mixing and deformations in mantle plumes. *Earth and Planetary Science Letters*, **196**, 1–15.

FITTON, J.G., SAUNDERS, A.D., NORRY, M.J., HARDARSON, B.S. & TAYLOR, R.N. 1997. Thermal and chemical structure of the Iceland plume: new insights from the alkaline basalts of the Snaefell volcanic centre. *Journal of the Geological Society*, London, **153**, 197–208.

FRAM, M.S. & LESHER, C.E. 1997. Generation and polybaric differentiation of East Greenland early Tertiary flood basalts. *Journal of Petrology*, **38**, 231–275.

FURMAN, T., BRYCE, J.G., KARSON, J. & IOTTI, A. 2004. East African Rift System (EARS) plume structure: insights from Quaternary mafic lavas of Turkana, Kenya. *Journal of Petrology*, **45**, 1069–1088.

FURMAN, T., KALETA, K.M. & BRYCE, J.G. 2006, Tertiary mafic lavas of Turkana, Kenya: constraints on temporal evolution of the EARS and the occurrence of HIMU volcanism in Africa. *Journal of Petrology* (doi: 10.1093/petrology/eg1009).

GEIST, D.J. 1992. An appraisal of melting processes and the Galápagos Hotspot: major- and trace-element evidence. *Journal of Volcanology and Geothermal Research*, **52**, 65–82.

GELDMACHER, J., HANAN, B.B., BLICHERT-TOFT, J., HARPP, K., HOERNLE, K., HAUFF, F., WERNER, R. & KERR, A.C. 2003. Hafnium isotopic variations in volcanic rocks from the Caribbean Large Igneous Province and the Galápagos hot spot tracks. *Geochemistry, Geophysics, Geosystems*, **4**, doi: 10.1029/2002GC000477.

GEORGE, R., ROGERS, N. & KELLEY, S. 1998. Earliest magmatism in Ethiopia: evidence for two mantle plumes in one flood basalt province. *Geology*, **26**, 923–926.

GIBSON, S.A., THOMPSON, R.N. & DICKIN, A.P. 2000. Ferropicrites: geochemical evidence for Fe-rich streaks in upwelling mantle plumes. *Earth and Planetary Science Letters*, **174**, 355–374.

GORDON, R.G. & JURDY, D.M. 1986. Cenozoic global plate motions. *Journal of Geophysical Research*, **91**, 12,389–12,406.

GRIPP, A.E. & GORDON, R.G. 2002. Young tracks of hotspots and current plate velocities. *Geophysical Journal International*, **150**, 321–361.

GURNIS, M., MITROVICA, J.X., RITSEMA, J. & VAN HEIJST, H.-J. (2000). Constraining mantle density structure using geological evidence of surface uplift rates: the case of the African Superplume. *Geochemistry, Geophysics, Geosystems*, **2**, Paper no. 1999GC000035.

HAILEAB, B., BROWN, F.H., MCDOUGALL, I. & GATHOGO, P.N. 2004. Gombe Group basalts and initiation of Pliocene deposition in the Turkana depression, northern Kenya and southern Ethiopia. *Geological Magazine*, **141**, 41–53.

HANAN, B.B. & SCHILLING, J.-G. 1997. The dynamic evolution of the Iceland mantle plume; the lead isotope perspective. *Earth and Planetary Science Letters*, **151**, 43–60.

HANAN, B.B. & SCHILLING, J.-G. 1989. Easter microplate evolution: Pb isotope evidence. *Journal of Geophysical Research*, **94**, 7432–7448.

HANAN, B., BLICHERT-TOFT, J., KINGSLEY, R. & SCHILLING, J.-G. 1999. Depleted Iceland mantle plume geochemical signature: Artifact of multicomponent mixing? *Geochemistry, Geophysics, Geosystems*, **1**, doi:10.1029/1999GC000009.

HARPP, K.S. & WHITE, W.M. 2001. Tracing a mantle plume: isotopic and trace element variations of Gal'pagos seamounts. *Geochemistry, Geophysics, Geosystems*, **2**, Paper no. 2000GC000137.

HART, S.R. 1984. A large-scale isotopic anomaly in the southern hemisphere. *Nature*, **309**, 753–757.

HART, W.K., WOLDEGABRIEL, G., WALTER, R.C. & MERTZMAN, S.A. 1989. Basaltic volcanism in Ethiopia: constraints on continental rifting and mantle interactions. *Journal of Geophysical Research*, **94**, 7731–7748.

HAWKESWORTH, C., KELLY, S., TURNER, S. & LE ROEX, A. 1998. Mantle processes during Gondwana breakup and dispersal. *Journal of African Earth Sciences*, **27**, 108–109.

HILL, R.I., CAMPBELL, I.H., DAVIES, G.F. & GRIFFITHS, R.W. 1992. Mantle plumes and continental tectonics. *Science*, **256**, 186–193.

HOERNLE, K., WERNER, R., MORGAN, J.P., GARBE-SCHÖNBERG, C.-D., BRYCE, J. & MRAZEK, J. 2000. Existence of complex spatial zonation in the Galápagos plume for at least 14 m.y. *Geology*, **28**, 435–438.

HOFMANN, A.W., JOCHUM, K.P., SEUFERT, M. & WHITE, W.M. 1986. Nb and Pb in oceanic basalts: new constraints on mantle evolution. *Earth and Planetary Science Letters*, **79**, 33–45.

HOFMANN, C., COURTILLOT, V., FÉRAUD, G., ROCHETTE, P., YIRGU, G., KETEFO, E. & PIK, R. 1997. Timing of the Ethiopian flood basalt event and implications for plume birth and global change. *Nature*, **389**, 838–841.

ISHIDA, M., MARUYAMA, S., SUETSUGU, D., MATSUZAKA, S. & EGUCHI, T. 1999. Superplume

Project: Towards a new view of whole Earth dynamics. *Earth Planets Space*, **51**, i–v.

JANNEY, P.E. & CASTILLO, P.R. 2001. Geochemistry of the oldest Atlantic oceanic crust suggests mantle plume involvement in the early history of the central Atlantic Ocean. *Earth and Planetary Science Letters*, **192**, 291–302.

JANNEY, P.E., LE ROEX, A.P., CARLSON, R.W. & VILJOEN, K.S. 2002. A chemical and multi-isotope study of the Western Cape melilitite province, South Africa: implications for the sources of kimberlites and the origin of the HIMU signature in Africa. *Journal of Petrology*, **43**, 2339–2370.

KEMPTON, P.D., FITTON, J.G., SAUNDERS, A.D., NOWELL, G.M., TAYLOR, R.N., HARDARSON, B.S. & PEARSON, G. 2000. The Iceland plume in space and time: a Sr–Nd–Pb–Hf study of the North Atlantic rifted margin. *Earth and Planetary Science Letters*, **177**, 255–271.

KENDALL, J.-M., STUART, G.W., EBINGER, C.J., BASTOW, I.D. & KEIR, D. 2005. Magma-assisted rifting in Ethiopia. *Nature*, **433**, 146–148.

KENT, A.J.R., BAKER, J.A. & WIEDENBECK, M. 2002. Contamination and melt aggregation processes in continental flood basalts: constraints from melt inclusions in Oligocene basalts from Yemen. *Earth and Planetary Science Letters*, **202**, 577–594.

KERANEN, K., KLEMPERER, S.L., GLOAUGEN, R. and the EAGLE working group (2004). Three-dimensional seismic imaging of a protoridge axis in the Main Ethiopian rift. *Geology*, **32**, 949–952.

KIEFFER, B., ARNDT, N., *ET AL.* 2004. Flood and shield basalts from Ethiopia: magmas from the African Superswell. *Journal of Petrology*, **45**, 793–834.

KURZ, M.D., CURTICE, J., LOTT, III, D.E. & SOLOW, A. 2004. Rapid helium isotopic variability in Mauna Kea shield lavas from the Hawaiian Scientific Drilling Project. *Geochemistry, Geophysics, Geosystems*, **5**, Q04G14, doi:10.1029/2002 GC000439.

KUSHIRO, I. 1996. Partial melting of a fertile mantle peridotite at high pressures: an experimental study using aggregates of diamond. *In*: BASU, A. & HART, S. (eds) *Earth Processes: Reading the Isotopic Code*. American Geophysical Union, 109–122.

LASSITER, J.C. & HAURI, E.H. 1998. Osmium-isotope variations in Hawaiian lavas: evidence for recycled oceanic lithosphere in the Hawaiian plume. *Earth and Planetary Science Letters*, **164**, 483–496.

MACDONALD, R. 1994. Petrological evidence regarding evolution of the Kenya Rift Valley. *Tectonophysics*, **236**, 373–390.

MACKENZIE, G., THYBO, H. & MAGUIRE, P. 2005. Crustal velocity structure across the Main Ethiopian Rift: results from two-dimensional wide-angle seismic modeling. *Geophysical Journal International*, **163**, 994–1006.

MAGUIRE, P.K.H., KELLER, G.R. *ET AL.* 2006. Crustal structure of the northern Main Ethiopian Rift from the EAGLE controlled-source survey: a snapshot of incipient lithospheric break-up. *In*: YIRGU, G., EBINGER, C.J. & MAGUIRE, P.K.H. (eds) *The Afar Volcanic Province within the East African Rift System*. Geological Society, London Special Publications, **259**, 269–291.

MAHATSENTE, R., JENTZSCH, G. & JAHR, T. 1999. Crustal structure of the Main Ethiopian Rift from gravity data: 3-dimensional modeling. *Tectonophysics*, **313**, 363–382.

MARTY, B., APPORA, I., BARRAT, J.-A., DENIEL, C., VELLUTINI, P. & VIDAL, P. 1993. He, Ar, Sr, Nd and Pb isotopes in volcanic rocks from Afar: evidence for a primitive mantle component and constraints on magmatic sources. *Geochemical Journal*, **27**, 223–232.

MARTY, B., PIK, R. & YIRGU, G. 1996. Helium isotopic variations in Ethiopian plume lavas: nature of magmatic sources and limit on lower mantle contribution. *Earth and Planetary Science Letters*, **144**, 223–237.

MOHR, P.A. 1962. The Ethiopian rift system. *Bulletin of the Geophysical Observatory*, **3**, 33–62.

MOHR, P. 1983. Ethiopian flood basalt province. *Nature*, **303**, 577–584.

MOHR, P. & ZANETTIN, B. 1988. The Ethiopian flood basalt province. *In*: MACDOUGALL, J.D. (ed.) *Continental Flood Basalts*. Kluwer Academic, Dordrecht, 63–110.

MONTELLI, R., NOLET, G., DAHLEN, F.A., MASTERS, G., ENGDAHL, E.R. & HUNG, S.-H. 2004. Finite-frequence tomography reveals a variety of plumes in the mantle. *Science*, **303**, 388–343.

MORGAN, W.J. 1972. *In*: SHAGAM, R. *ET AL.* (eds) *Studies in Earth and Space Science*. Geological Society of America Memoir, **132**.

MUKHOPADHYAY, S., LASSITER, J.C., FARLEY, K.A. & BOGUE, S.W. 2003. Geochemistry of Kauai shield-stage lavas: Implications for the chemical evolution of the Hawaiian plume. *Geochemistry, Geophysics, Geosystems*, **4**(1), 1009, doi:10.1029/2002 GC000342.

NI, S., TAN, E., GURNIS, M. & HELMBERGER, D. 2002. Sharp sides to the African superplume. *Science*, **296**, 1850–1852.

NYBLADE, A.A., OWENS, T.J., GURROLA, H., RITSEMA, J. & LANGSTON, C.A. 2000. Seismic evidence for a deep upper mantle thermal anomaly beneath east Africa. *Geology*, **28**, 599–602.

PEATE, D.W., HAWKESWORTH, C.J. & MANTOVANI, M.S.M. 1992. Chemical stratigraphy of the Paraná lavas (South America): classification of magma types and their spatial distribution. *Bulletin of Volcanology*, **55**, 119–139.

PECCERILLO, A., BARBERIO, M.R., YIRGU, G., AYALEW, D., BARBIERI, M. & WU, T.W. 2003. Relationship between mafic and peralkaline silicic magmatism in continental rift settings: a petrological, geochemical and isotopic study of the Gedemsa volcano, central Ethiopian rift. *Journal of Petrology*, **44**, 2003–2032.

PIK, R., DENIEL, C., COULON, C., YIRGU, G., HOFMANN, C. & AYALEW, D. 1998. The northwestern Ethiopian Plateau flood basalts: classification and spatial distribution of magma types. *Journal of Volcanology and Geothermal Research*, **81**, 91–111.

PIK, R., DENIEL, C., COULON, C., YIRGU, G. & MARTY, B. 1999. Isotopic and trace element signatures of Ethiopian flood basalts; evidence for plume-lithosphere interactions. *Geochimica et Cosmochimica Acta*, **63**, 2263–2279.

PIK, R., MARTY, B. & HILTON, D.R. 2006. How many mantle plumes in Africa? The geochemical point of view. *Chemical Geology*, **226**, 100–114.

RICHARDS, M.A., DUNCAN, R.A. & COURTILLOT, V.E. 1989. Flood basalts and hot-spot tracks: plume heads and tails. *Science*, **246**, 103–107.

RITSEMA, J., VAN HEIJST, H.J., & WOODHOUSE, J.H. 1999. Complex shear wave velocity structure imagedc beneath Africa and Iceland. *Science*, **286**, 1925–1928.

ROGERS, N., MACDONALD, R., FITTON, J.G., GEORGE, R., SMITH, M. & BARREIRO, B. 2000. Two mantle plumes beneath the East African rift system: Sr, Nd and Pb isotope evidence from Kenya Rift basalts. *Earth and Planetary Science Letters*, **176**, 387–400.

ROGERS, N. 2006. Basaltic magmatism and the geodynamics of the African Rift. *In*: YIRGU, G., EBINGER, C.J. & MAGUIRE, P.K.H. (eds) *The Afar Volcanic Province within the East African Rift System.* Geological Society, London Special Publications, **259**, 77–93.

ROMANOWICZ, B. & GUNG, Y. 2002. Superplumes from the core-mantle boundary to the lithosphere; implications for heat flux. *Science*, **296**, 513–516.

RUDNICK, R.L., MCDONOUGH, W.F. & CHAPPELL, B.W. 1993. Carbonatite metasomatism in the northern Tanzanian mantle: petrographic and geochemical characteristics. *Earth and Planetary Science Letters*, **114**, 463–475.

SAAL, A.E., HART, S.R., SHIMIZU, N., HAURI, E.J. & LAYNE, G.D. 1998. Pb isotopic variability in melt inclusions for oceanic island basalts, Polynesia. *Science*, **282**, 1481–1484.

SAMUEL, H. & FARNETANI, C.G. 2003. Thermochemical convection and helium concentrations in mantle plumes. *Earth and Planetary Science Letters*, **207**, 39–56.

SCARSI, P. & CRAIG, H. 1996. Helium isotope ratios in Ethiopian Rift basalts. *Earth and Planetary Science Letters*, **144**, 505–516.

SCHILLING, J.-G., HANAN, B.B., MCCULLY, B., KINGSLEY, R.H. & FONTIGNIE, D. 1994. Influence of the Sierra Leone mantle plume on the equatorial Mid-Atlantic Ridge: a Nd–Sr–Pb isotopic study. *Journal of Geophysical Research*, **99**, 12005–12028.

SCHILLING, J.-G., KINGSLEY, R.H., HANAN, B.B. & MCCULLY, B.L. 1998. Nd–Sr–Pb isotopic variations along the Gulf of Aden: evidence for Afar mantle plume-continental lithosphere interaction. *Journal of Geophysical Research*, **97**, 10927–10966.

SHAW, J.E., BAKER, J.A., MENZIES, M.A., THIRLWALL, M.F. & IBRAHIM, K.M. 2003. Petrogenesis of the largest intraplate volcanic field on the Arabian Plate (Jordan): a mixed lithosphere–asthenosphere source activated by lithospheric extension. *Journal of Petrology*, **44**, 1657–1679.

SILVER, P., RUSSO, R.M. & LITHGOW-BERTELLONI, C. 1998. Coupling of South American and African plate motion and plate deformation. *Science*, **279**, 60–63.

SPÄTH, A., LE ROEX, A.P. & OPIYO-AKECH, N. 2001. Plume-lithosphere interaction and the origin of continental rift-related alkali volcanism – the Chyulu Hills volcanic province, southern Kenya. *Journal of Petrology*, **42**, 765–787.

STEWART, K. & ROGERS, N. 1996. Mantle plume and lithosphere contributions to basalts from southern Ethiopia. *Earth and Planetary Science Letters*, **139**, 195–211.

SUN, S.-S. & MCDONOUGH, W.F. 1989. Chemical and isotopic systematics of oceanic basalts: implications for mantle composition and processes. *In*: SAUNDERS, A.D. & NORRY, M.J. (eds) *Magmatism in the Ocean Basins.* Geological Society, London, *Special Publications*, **42**, 313–345.

THIRLWALL, M.F. 1995. Generation of the Pb isotopic characteristics of the Iceland plume. *Journal of the Geological Society*, London, **152**, 991–996.

THIRLWALL, M.F. 2002. Multicollector ICP-MS analysis of Pb isotopes using a ^{207}Pb–^{204}Pb double spike demonstrates up to 4000 ppm/amu systematic errors in Tl-normalization. *Chemical Geology*, **184**, 255–279.

THOMPSON, P.M.E., KEMPTON, P.D., WHITE, R.V., KERR, A.C., TARNEY, J., SAUNDERS, A.D., FITTON, J.G. & MCBIRNEY, A. 2004. Hf–Nd isotope constraints on the origin of the Cretaceous Caribbean plateau and its relationship to the Galápagos plume. *Earth and Planetary Science Letters*, **217**, 59–75.

TIBERI, C., EBINGER, C., BALLU, V., STEWART, G. & OLUMA, B. 2005. Inverse models of gravity data from the Red Sea–Aden–East African rifts triple junction zone. *Geological Society of America Bulletin*, **163**, 775–787.

TIBERI, C., EBINGER, C., BALLU, V., STUART, G. & OLUMA, B. 2005. Inverse models of gravity data from the Red Sea-Aden-East African Rifts triple junction zone. *Geophysical Journal International*, **163**, 775–787.

TODT, W., CLIFF, R.A., HANSER, A. & HOFMANN, A.W. 1996. Evaluation of a 202Pb-205Pb double spike for high precision lead isotope analysis. *In*: BASU, A. & HART, S. (eds) *Earth Processes: Reading the Isotopic Code.* American Geophysical Union, 429–437.

TRUA, T., DENIEL, C. & MAZZUOLI, R. 1999. Crustal control in the genesis of Plio-Quaternary bimodal magmatism of the Main Ethiopian Rift (MER): geochemical and isotopic (Sr, Nd, Pb) evidence. *Chemical Geology*, **155**, 201–231.

VETEL, W. & LE GALL, B. 2006. Dynamics of prolonged continental extension in magmatic rifts: the Turkana Rift case study (Northern Kenya). *In*: YIRGU, G., EBINGER, C.J. & MAGUIRE, P.K.H. (eds) *The Afar Volcanic Province within the East African Rift System.* Geological Society, London, *Special Publications*, **259**, 209–233.

VIDAL, P., DENIEL, C., VELLUTINI, P.J., PIGUET, P., COULON, C., VINCENT, J. & AUDIN, J. 1991.

Changes of mantle sources in the course of a rift evolution: the Afar case. *Geophysical Research Letters*, **18**, 1913–1916.

WASYLENKI, L.E., BAKER, M.B., KENT, A.J.R. & STOLPER, E. 2003. Near-solidus melting of the shallow upper mantle: partial melting experiments on depleted peridotite. *Journal of Petrology*, **44**, 1163–1191.

WEERARATNE, D.S., FORSYTH, D.W., FISHER, K.M. & NYBLADE, A.A. 2003. Evidence for an upper mantle plume beneath the Tanzanian Craton from Rayleigh wave tomography. *Journal of Geophysical Research*, **108**, doi: 10.1029/2002JB002273.

WHITE, W.M., MCBIRNEY, A.R. & DUNCAN, R.A. 1993. Petrology and geochemistry of the Galápagos Islands: portrait of a pathological mantle plume. *Journal of Geophysical Research*, **98**, 19,533–19,563.

WHITE, W.M., ALBARÈDE, F. & TÉLOUK, P. 2000. High-precision analysis of Pb isotopic ratios using multicollector ICP-MS. *Chemical Geology*, **167**, 257–270.

WHITE, R.S., & MCKENZIE, D.M. 1995. Mantle plumes and flood basalts, *Journal of Geophysical Research*, **100**, 17,543–17,585.

WOLDEGABRIEL, G., ARONSON, J.L. & WALTER, R.C. 1990. Geology, geochronology, and rift basin development in the central sector of the Main Ethiopian Rift. *Geological Society of America Bulletin*, **102**, 439–458.

WOLFENDEN, E., EBINGER, C., YIRGU, G., DEINO, A. & AYALEW, D. 2004. Evolution of the northern Main Ethiopian Rift: birth of a triple junction. *Earth and Planetary Science Letters*, **224**, 213–228.

ZHAO, D. 2001. Seismic structure and origin of hotspots and mantle plumes. *Earth and Planetary Science Letters*, **192**, 251–265.

ZUMBO, V., FÉRAUD, G., VELLUTINI, P., PIGUET, P. & VINCENT, J. 1985. First $^{40}Ar/^{39}Ar$ dating on Early Oligocene to Plio-Pleistocene magmatic events of the Afar–Republic of Djibouti. *Journal of Volcanology and Geothermal Research*, **65**, 281–295.